FLEXIBLE POLYMER DISPLAY TECHNOLOGIES

by

Ali Osman Sevim

B.S., Electronics Engineering, Kadir Has University, 2005

Submitted to the Institute for Graduate Studies in

Science and Engineering in partial fulfillment of

the requirements for the degree of

Master of Science

Graduate Program in System and Control Engineering

Boğaziçi University

2008

FLEXIBLE POLYMER DISPLAY TECHNOLOGIES

APPROVED BY:

Assist. Prof. Şenol Mutlu ……

(Thesis Supervisor)

Assist. Prof. Amitav Sanyal ……

Assist. Prof. Arda Deniz Yalçinkaya ……

DATE OF APPROVAL: 29.02.2007

ACKNOWLEDGEMENTS

This thesis was done under the supervision of Assist. Prof. Şenol Mutlu in Department of Electrical and Electronics Engineering. I would like to express my sincere gratitude to my advisor, Dr. Şenol Mutlu, for providing me this chance to work on this exciting and interdisciplinary research and for his extensive guidance, valuable discussions and great interest.

I also want to thank my committee members, Assist. Prof. Arda Deniz Yalçinkaya and Assist. Prof. Amitav Sanyal for their collaboration. Especially, I would like to thank Dr. Sanyal for his insightful discussions and assistance in the laboratory works of the fabrication.

I wish to thank Orhan Mert and my other friends in BETA laboratory for their friendship and collaborations during my study.

Special thanks for Prof. Feza Kerestecioğlu for his valuable conversations and supports since undergraduate years in Kadir Has University.

Finally, I wish to thank my precious wife, Serap Becit Sevim, for her continuous support and encouragement. And I want to express my sincere thanks to our families for their patient love and supports.

This work has been fully supported by Scientific & Technological Research Council of Turkey (TUBITAK) under the project name INPOMIS-INtegrated Polymer MIcro Systems with project number 106E013. The financial support of TUBITAK in this project is gratefully acknowledged.

ABSTRACT

FLEXIBLE POLYMER DISPLAY TECHNOLOGIES

Conjugated polymers are semiconductors that have attracted increasing attention especially in the last decade, which enabled fabrication of polymer light emitting diodes (PLEDs), polymer circuits, polymer photodetectors and solar cells. They offer flexibility, simplicity and feasibility in fabrication. They lead to a technology which can monolithically integrate the devices mentioned above to micro-electromechanical systems (MEMS). Polymer photonic devices have lower performance compared to inorganic counterparts and have degradation problem. They still need fabrication refinements, more characterization, testing and product treatments for performance improvement. This research presents a novel method as a post-fabrication treatment that improves the performance of polymer light emitting diodes. Investigated PLED is made of indium tin oxide (ITO), poly(3,4-ethylenedioxythiophene) poly(styrenesulfonate) (PEDOT:PSS), poly[2-methoxy-5-(2'-ethyl-hexyloxy)-1,4-phenylene vinylene] (MEH-PPV) and aluminum. Fabrication process of the polymer light emitting diode is systematically evaluated. Vacuum heat treatment is performed at 130 ºC for one hour and electric field treatment is realized with negative voltages. Post fabrication heat treatment restores the light emitting function of PLEDs, which have failed due to absorbed oxygen and humidity during fabrication realized in normal room conditions. Electric field treatment lowers the turn-on voltage of PLEDs from 11 volts to 4 volts after treatment with -1 volt, when they are used as light emitting devices. Also it improves open circuit voltages and short circuit currents by an order of magnitude when they are used as photo-detectors or photocells after packaging. Electric field treatment applied after the thermal treatment also improves the uniformity of the devices.

ÖZET

ESNEK POLİMER EKRAN TEKNOLOJİLERİ

Özellikle son on yılda giderek artan ilgi toplayan konjüge polimer yarıiletkenler ışık yayan polimer diyotlar (PLED), polimer devreler, polimer foto algılayıcılar ve güneş pillerinin üretimini mümkün kılmaktadırlar. Fabrikasyonda esneklik, basitlik ve etkinlik sağlamaktadırlar. Yukarıda bahsedilen aygıtların mikro elektromekanik sistemlere (MEMS) monolitik olarak tümleştirilmelerini sağlayan bir teknolojiye önderlik etmektedirler. Polimer ışıksal gereçler inorganik rakiplerine kıyasla daha az performansa sahiptirler ve bozulma problemleri vardır. Daha iyi başarım için hala üretim iyileştirmesi, karakterizasyon, test ve ürün tedavisine ihtiyaçları vardır. Bu araştırma polimer ışık diyotların performanslarını arttıran, özgün bir üretim sonrası tedavi yöntemi sunmaktadır. İncelenen PLED indiyum tin oksit (ITO), poly(3,4-ethylenedioxythiophene) poly (styrenesulfonate) (PEDOT:PSS), poly[2-methoxy-5-(2'-ethyl-hexyloxy)-1,4-phenylene vinylene] (MEH-PPV) ve alüminyumdan yapılmıştır. PLED üretim süreci sistematik olarak incelenmiştir. Isı vakum tedavisi 130 Cº'de bir saat ve elektrik alanı tedavisi ise eksi voltajlarla gerçekleştirilmiştir. Üretim sonrasındaki ısı tedavisi, olağan oda koşullarında gerçekleştirilen üretim esnasında oksijen ve neme maruz kalmasından dolayı bozulan PLED'lerin ışık yayma özelliğini geri getirmektedir. Elektrik tedavisi sonuçları göstermektedir ki PLEDler ışık yayan diyot olarak kullanıldıklarında ve -1 volt ile tedavi edilmişler ise çalışmaya başlama eşiği 11 volttan 4 volta düşmektedir. Yine elektrik tedavisi sonuçları göstermektedir ki PLEDler paketlemeden sonra foto algılayıcı veya güneş hücresi olarak kullanıldıklarında ise açık devre gerilimleri ve kısa devre akımları on kat iyileşmektedir. Ayrıca ısıl tedavisi sonrası uygulanmış elektrik alanı tedavisi aygıtların düzgünlüğünü iyileştirmektedir.

TABLE OF CONTENTS

LIST OF FIGURES

LIST OF TABLES

LIST OF SYMBOLS/ABBREVIATIONS

Al	Aluminum
Ag	Silver
As	Arsenic
Au	Gold
c	Speed of light
C	Carbon
Ca	Calcium
Cd	Cadmium
cm^2	Centimeter square
Cr	Chrome
Cu	Copper
CuPc	Copper phthalocyanine
eV	Electron volt
E	Energy
E_g	Energy gap
E_b	Energy barrier
Fe	Iron
h	Plank's constant
H	Hydrogen
Hg	Mercury
HMDS	Hexamethyldisilazane
Hz	Hertz
IPA	Isopropyl alcohol
ITO	Indium tin oxide
J	Joule
K	Potassium
kg	Kilogram
Li	Lithium

MEH-PPV	poly[2-methoxy-5-(2'-ethyl-hexyloxy)-1,4-phenylene vinylene]
mCd	Millicandela
mg	Milligram
Mg	Magnesium
ml	Milliliter
mlx	Millilux
mm	Millimeter
mV	Millivolt
mW	Milliwatt
nA	Nanoampere
nm	Nanometer
Na	Sodium
Ni	Nickel
NPB	N, N'-diphenyl-N, N'-bis (1-naphthylphenyl)-1, 1'-biphenyl-4, 4'-diamine
PANI	Polyaniline
Pb	Lead
PEDOT	poly (3,4-ethylenedioxythiophene)
PEDOT:PSS	poly(3,4-ethylenedioxythiophene) poly(styrenesulfonate)
PET	Polyethylene terephthalate
pH	Power of hydrogen
PPV	poly (p-phenlyne vinylene)
Pt	Platinum
PSS	poly (styrene sulfonate)
rpm	Revolutions per minute
s	Second
Ti	Titanium
TMAH	Tetramethylammonium hydroxide
TPD	N, N'-diphenyl-N, N'-bis (3-methylphenyl)-1,1'-biphenyl-4,4'-diamine
V	Volt
ZnO	Zinc oxide

A	Angstrom
˚ C	Celsius degree
λ	Lambda
μ	Micrometer
η_{ext}	External quantum efficiency
η_{cp}	Coupling efficiency
η_{int}	Internal quantum efficiency
η_{eh}	Efficiency of electron and hole balance
η_{st}	Ratio of the number of singlets to triplets
η_{pl}	Photoluminescence quantum efficiency
%	Percent

AM	Active matrix
CAD	Computer aided design
DC	Direct current
DI	Deionized
EL	Electroluminescent
ETL	Electron transfer layer
FOIS	Fiber optic integrating sphere
HOMO	Highest occupied molecular orbital
HT	Hole-transporting
HTL	Hole transport layer
IS	Integrating sphere
MEMS	Micro electro mechanical systems
LED	Light emitting diodes
LUMO	Lowest unoccupied molecular orbital
OE	Organic electronic
OLED	Organic light emitting diode
PDMS	Polydimethylsiloxane
PC	Personal computer
PIC	Programmable integrated circuit
PL	Photoluminescence

PLED	Polymer light emitting diode
PM	Passive matrix
PPI	Pulse per inch
PR	Photoresist
RIE	Reactive ion etching
SM	Small molecule
SMOLED	Small molecular organic light emitting diode
T-T	Triplet-triplet
UV	Ultraviolet
UV-NIR	Ultraviolet to near infrared
WF	Work function

1. INTRODUCTION

1.1. Motivation

Organic light emitting diode (OLED) displays are thin film devices, which have the advantages of low power consumption [1], mechanical flexibility, low-cost production, manufacturing advantage, and monolithic integration ability with flexible substrate based devices [2]. The traditional production in microelectronics and micro electro mechanical systems (MEMS) is complex and require high investment because it needs high-tech clean rooms whose costs are around millions of dollars [3]. However, scientists and engineers are able to produce numerous devices and systems, electrical or mechanical, in a faster and cheaper way by using polymers with different properties. In the applications of MEMS in biology, SU-8 [4], polydimethylsiloxane (PDMS) [5], parylene [6,7] are used as structural materials and smart materials, which are sensitive to temperature, light, pH, and glucose, are used to develop micro-fluid based biosensors [8] and chemical and basic biological analyzers [9]. Likewise, polymer based systems can be produced by using self-assembled monolayer, PDMS and soft lithography method [10]. By the same way, light emitting diodes [11], photocells [10], electronic polymer circuits [13], and flexible displays [14] are manufactured simply by using soluble conjugated polymers [15].

In the past ten years, electronic devices made by organic materials attracted increasing attention due to advantages mentioned above. In addition to important properties of polymeric materials, the variety of plastic based devices is increasing drastically. This makes organic electronic (OE) market charming and profitable. The forecast about the future of the organic electronic market supports this spectacular evolution. Predictions are given in Figure 1.1 [16] from Nanomarkets, a company providing research services and reports for the analysis of thin film, organic and printable electronics related industry, market and technology. Organic electronic devices are expected to find application especially in display sector. Displays made of OLED have broad color scale, wide viewing angle and high contrast [17]. Passive matrix (PM), generally monochrome, displays are used particularly in mobile devices due to their low power consumption, lightweight, transparency and large area applicability [18]. Because

the organic light emitting diodes are thin, have increasing efficiencies and simple fabrication process, they have been used as a backplane flat panels or as a general purpose display with matrix structure [19].

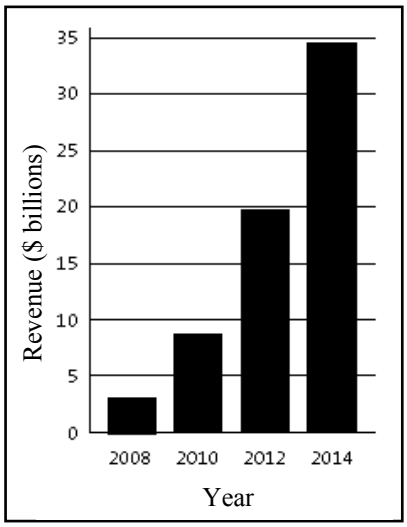

Application	Revenue ($ billions)
Displays	13,815.0
Signage	493.2
Lighting	1,200.0
Backplanes	2,764.2
Sensors	1,600.0
RFIDs	11,073.3
PV	127.2
Memory	1,500.0
Toys and novelties	1,400.0
Other	468.3
Total	**34,441.3**

Figure 1.1. Forecasts for OE market (left), revenue by application in 2014 (right) [16]

On the other hand, OE devices have another potential to realize a system that can integrate all the devices mentioned above monolithically. They can even be integrated to polymer MEMS to acquire sensing and actuation [20, 21].

However, compared to their inorganic counterparts, polymer semiconducting devices today have relatively lower performances, less reliabilities and shorter lifetimes [22, 23, 24]. The main reason for this is the fast degradation nature of these polymers under oxygen and water vapor environment. Therefore, polymer semiconducting devices still need more research on the refinement of their fabrication, characterization and testing of their performances and post fabrication treatments for performance improvement.

Several groups have studied performance improvement and stability of organic materials used in polymer light emitting devices [25-28] and solar cells [29, 30]. In these studies, in order to increase the performance of polymer or to prevent contamination of semiconducting devices all fabrication steps are done in an inert environment like nitrogen or argon. Similarly, they have applied different treatment methodologies at some point of the fabrication process like ultraviolet (UV) ozone or chemical treatments applied to indium tin oxide (ITO) or conducting polymers. [25-30] However, all these extra

precautions make the production harder and more costly. This research presents a new method, a post-fabrication heat treatment followed by an electric field treatment, and its influences on the performance of ITO / poly(3,4-ethylenedioxythiophene) poly(styrenesulfonate) (PEDOT:PSS) / poly[2-methoxy-5-(2'-ethyl-hexyloxy)-1,4-phenylene vinylene] (MEH-PPV) / aluminum (Al) polymer light emitting diodes (PLEDs). Previously, a similar post fabrication treatment has been shown to work on polymer solar cells [31] or electroluminescent devices based on dendrimer, small molecules devices and polymers [32, 33]. However, this is the first time a post fabrication thermal treatment of polymers followed by an electric field treatment in reverse bias is applied to PLEDs and shown that it modifies their turn-on voltages and improves their photovoltaic properties.

In this thesis, in the first part of this chapter fundamental knowledge about PLED is given. In second chapter, the fabrication steps of polymer light emitting diodes are given in detail. External factors, which influence fabrication process, are defined and their effects are illustrated additionally. This is followed by the explanation of the details of the post fabrication thermal and electric field treatments. The effects of the heat treatment by itself and the heat treatment followed by electric field treatment on turn-on voltages and photovoltaic properties of PLEDs are presented. The results are analyzed and discussed and possible future works are given in the last chapter.

1.2. History of Polymer Electroluminescent Devices

Today, organic electronics hold significant challenge in commercial market and used in the variety of applications like organic lasers, fuel cell, batteries, biologic sensors, photo detectors, flexible circuits and especially in displays [2, 11-15]. Although, the first observation of light from the organic material is obtained in 1953 [34, 35] and direct current (DC) version in 1963 [36], the electroluminescence from inorganic matters was known since 1907 [37-39]. Due to high operating voltage levels, low light outputs and physical inefficiencies (thick) [40], there was not any commercialized product until 1999 when Pioneer announced that they used small molecular organic light emitting diode (SMOLED) based display in consumer electronics goods [41]. At these years, SK Display Coorporation announced the first active matrix (AM) small molecule display manufactured for Kodak cameras [42], Figure 1.2.a.

On the other hand, similar fast progress is achieved in another type of organic light emitting diodes, PLEDs. Most outstanding discovery is that the conductivity of polymers was increased by tens order of magnitude in 1977 [43, 44] by the invention of conjugated polymers which is awarded the Nobel Prize in chemistry in 2000. By iodine doping of polyacetylene conductivity was increased and the polymeric materials gain importance and find huge range of applications especially in electroluminescence devices after the discovery of photo-excitation [45, 46]. Then, research was generally focused to enhance the chemical properties and efficiencies of light emitting devices and, in 1990, the luminescent polymer, poly (p-phenlyne vinylene) (PPV) was developed. PPV was sandwiched between transparent electrode ITO and thermally evaporated Al by spin coating method since PPV can be solution-processed [47, 48, 49]. Consecutive investigations made the PPV high efficient, excellently soluble in common organic solvents [50, 51], soluble at higher molecular weights and able to run at low voltages with longer lifetimes [52-54]. In 2002, PPV based PLED displays were commercially available from Philips. That was the first conjugated polymer-based electroluminescent display on the market, Figure 1.2.b. [55]. These discoveries opened a new perception to the display technologies. New polymers, oligomers and small molecules have been developed in addition to novel fabrication methodologies. And recently, in 22nd January 2008 Poymervision has announced the commercial launch of Radius®, shown in Figure 1.2.c. which is a third generation (3G) multimedia mobile phone with flexible grayscale 5" display and with six times longer battery life, in mid 2008. [56]

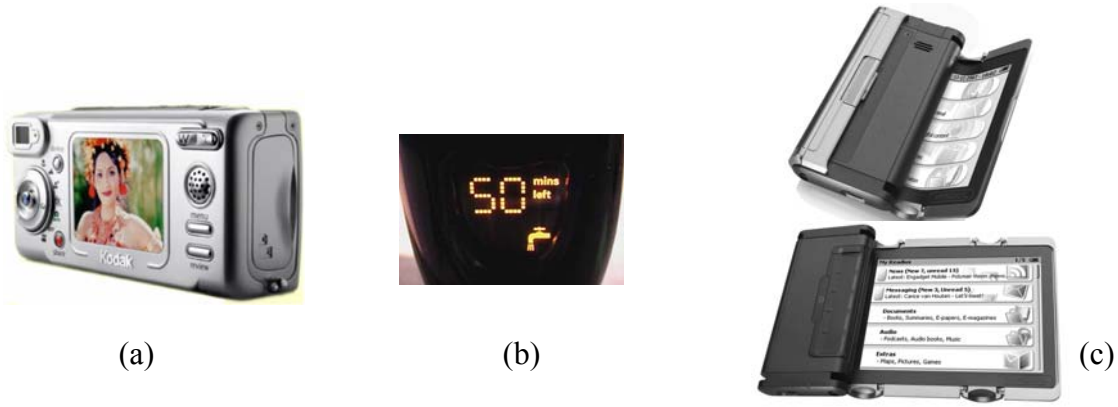

(a) (b) (c)

Figure 1.2. Kodak Camera with AM OLED (a), Philips Electronic razor with PLED (b), 3G mobile device by Polymervision with flexible active matrix 5" display (c)

Polymeric electronic materials and devices find wide range of applications especially in human machine interfaces since they are light-weighted, easy to manufacture, less consumption of raw material, flexible and resistive against corrosion, However, there are still some problems about fabrication, lifetime, stability and repeatibilty of polymer-based devices because of their sensitivity to oxygen and water. More research is still needed in this area.

1.3. Conduction in Polymers

Conventionally, polymers, materials that have repeating molecular units (generally carbon based matters), are used as insulators especially in industrial applications. These insulator materials are called saturated polymers, Figure 1.3. The valence electron of each carbon is bonded with four near atoms and hybridization occurs in sp^3 configuration. For that reason, they have fully saturated orbital structure and they have wide energy gaps for electrical conduction.

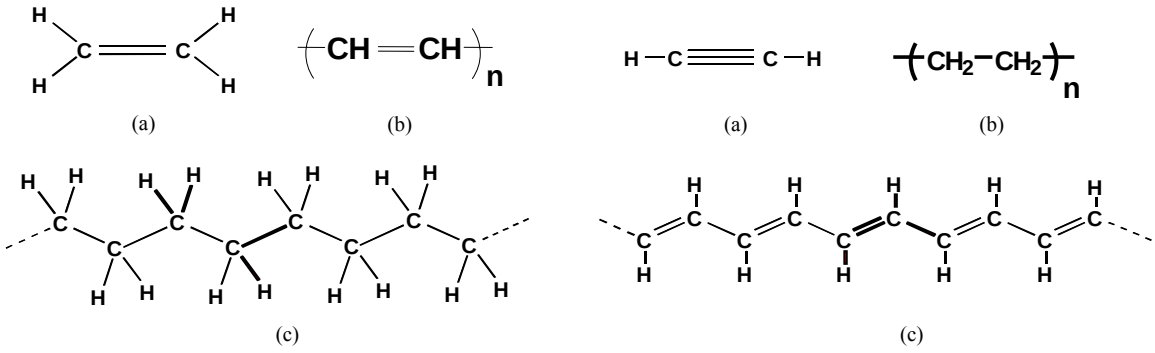

Figure 1.3. (a) Repeating units, (b) molecular structures and (c) chain structures of saturated polymer Polyethylene (left), transparent conductive polyacetylene (right)

On the other hand, in conjugated polymers, where single and double or triple bonds alternate through the polymer backbone (assume oriented with x axis), each carbon atom is bounded with three neighboring atom and the sp^2 p_z configuration is formed. The organic molecule's mutual overlap of the p_z orbital along the conjugation line forms π-bands, Figure 1.4. Depending on whether the π bands are fully or partly filled the conjugated polymer holds semiconducting or metallic properties. In the semiconductors, 2.3 – 3 eV energy gap (E_g) is observed between the highest occupied molecular orbital (HOMO) (sometimes called bonding orbital or valence band and denoted by π), and the lowest unoccupied molecular orbital (LUMO) (sometimes called non-bonding orbital or

conduction band and denoted by π^*) [57]. Variations on the energy gap change the magnitude of light energy and color of the light.

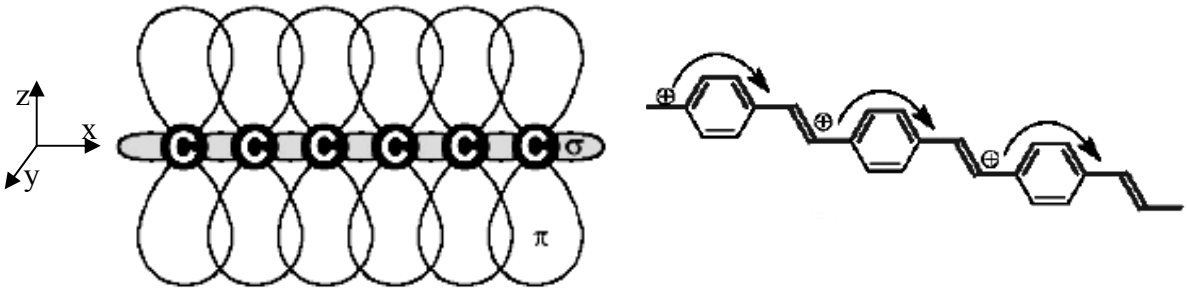

Figure 1.4. Mutual overlaps of orbitals along conjugation (left), electrical conduction in conjugated polymers (right)

Moreover depending on the distance between carbon atoms, electron cloud density changes and the electronic structure of materials varies [58, 59]. The length of alternating segment can also be changed by adding impurities and by that way reciprocal density extending over the entire conjugation path will be changed. The light intensity obtained from shorter length molecules is higher than the longer molecules.

1.4. Electroluminescence in Polymer Devices

Energy gap levels Eg of the conjugated polymers are suitable for photonics applications and they have excellent mechanical (flexible, thin) and manufacturing properties; therefore, their usages in optoelectronics devices have been growing steadily. The most widely used electroluminescent polymer is poly (phenylene vinylene) or PPV. At the beginning, PPV was insoluble and emitted yellow–green light since it had a badgap of 2.5 eV [48]. By adding alkoxy elements to 2 and 5 positions of PPV, (poly (2-methoxy-5-(2 -ethyl) hexyloxy-p-phenylene vinylene), or MEH:PPV) it becomes soluble in general non polar solvents such as toluene, xylene and the E_g can be varied from 2.5 to 2.1 eV. Unlike small molecule (SM) organic materials, electroluminescent polymers are soluble and their depositions are easier.

Polymer light emitting device is composed of a thin film of an electroluminescent polymer (light generating material under electric field) between thin films of two electrodes. In this thesis poly (2-methoxy-5- (2 -ethyl) hexyloxy-p-phenylene vinylene)

MEH:PPV is used between a conductive polymer and a metallic cathode. Conductive polymer is used as a hole transport layer (HTL) to improve efficiency.

On biasing the polymer devices in forward region, as shown in Figure 1.5, electrons are injected from the cathode. Similarly holes from the anode are inserted into the polymer layer. The cathode injects electrons in LUMO, and the anode injects holes to HOMO. The negative electrode is selected from low work function metals to facilitate the electron injection. Similarly anode electrode has a high work function so that it can inject holes to the polymer layer.

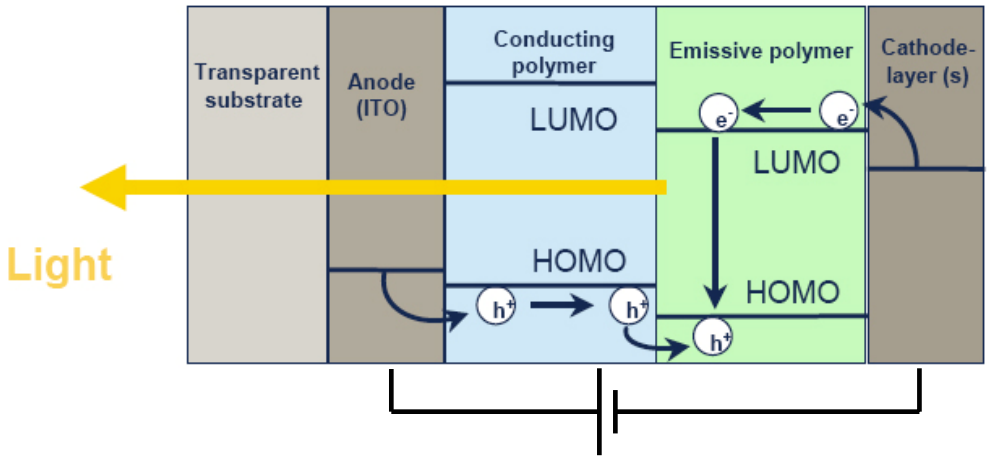

Figure 1.5. Energy diagram for polymer light emitting diode

The injected charges in the polymer can move from one electrode to another due to electric field. If the electrons are recombined with holes, an exciton is formed [60, 61]. Depending on the spin statistics, the excitons might be in two states; singlet or triplet. Triplets are formed due to spin-symmetric excitons and they can not decay radiatively to ground state. [62] Moreover, only one of two triplet excitons can introduce fluorescent emission, as shown in Figure 1.6. Because of the overall spin quantum parameters between the two states, the theoretical maximum internal quantum efficiency of diodes is 25 % for small molecule devices without modification. Intersystem crossing is seen from singlet exciton to lowest state of triplet position, and generally is not observed in conjugated polymers. In triplet-triplet (T-T) annihilation two triplets combine and form a singlet and a ground state. This process decreases the quantum efficiency when the junction is run at high currents. To eliminate the effect either triplet lifetimes must be shortened or dopant aggregation in thin film must be decreased. [63] Nevertheless, some studies report

efficiencies beyond this theoretical ratio as high as 80 to 100 % [64]. Photoluminescence (PL) (the light generation under optical radiation) can be achieved by light without recombination through successively decaying excitons.

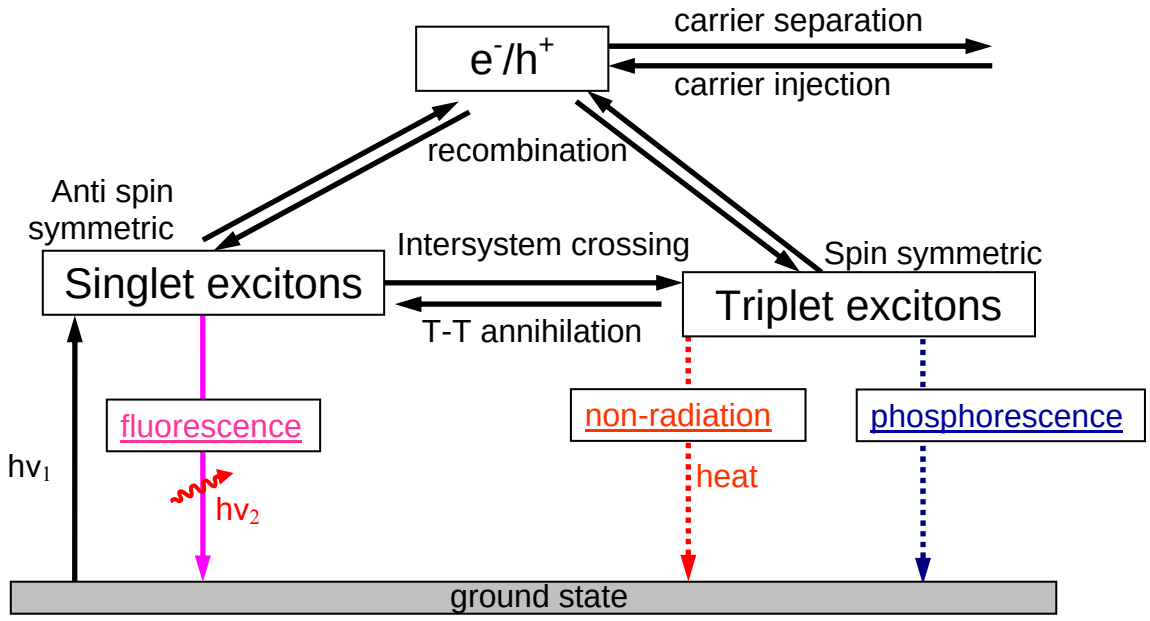

Figure 1.6. Physics of photo excitation

In addition, if the junction is reverse biased, because of the high energy barriers charges can not be injected into the polymers. The charges injected in the reverse bias forms the reverse bias current which is negligible compared to forward bias current. The ratio of the forward bias current to the reverse bias current of the light emitting polymer diode made up of MEH-PPV is reported as 10^6 [65].

1.5. Efficiency of PLEDs

Efficiency is the key performance measure for the light emitting devices. Inefficient device not only consumes more energy also degrades itself by heating, which decreases its operation time. PLED power efficiency is the ratio of total light power emitted from the device to the applied electrical power. This ratio can also be referred as external quantum efficiency (η_{ext}). External quantum efficiency is the overall multiplication of the efficiencies of certain stages that light has to pass through in order to become visible on the surface of the device starting from charge injection and ending at the emission from the

outer packaging layer. Fundamental equation for the external quantum efficiency of an organic light emitting diodes (LED) can be written as below (1.1).

$$\eta_{ext} = \eta_{cp} \cdot \eta_{int} = \eta_{cp} \cdot \eta_{eh} \cdot \eta_{st} \cdot \eta_{pl} \quad (1.1)$$

Coupling efficiency (η_{cp}) is a coefficient that measures how much light can escape from the active area of the device, Figure 1.7. It is generally smaller than 100 % due to internal reflections, which depends on the reflection indices of the substrate, and the reflectivity of back plane material. For example for Polyethylene terephthalate (PET) substrate, if n=1.5 (reflective indices), the η_{cp} can be found as 22 % from the equation 1.2.

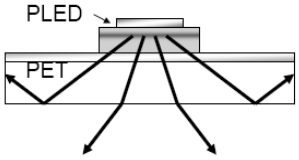

Figure 1.7. η_{cp} is a measure of light extraction from the active area inside the device

$$\eta_{cp} = 0.5 \times (1 / n^2) \quad (1.2)$$

Cathode reflectors [66] or micro lenses attached to the PET surface can always be used to increase coupling efficiency. However, this is not the topic of this work.

The internal quantum efficiency (η_{int}) is the general name given to the product of efficiency coefficients defining the quality of energy conversion inside the device. The constant (η_{eh}) is used as a measure for the balance between electron and hole injections. In other terms, the ratio of the electrons and holes which recombine together gives η_{eh}. This ratio can be optimized by varying the thicknesses of the HTL and electron transfer layer (ETL). However, by changing the thickness in order to improve the efficiency, turn-on voltage increases and vice versa. Excess injection of holes in polymer junction decreases efficiency and results in heat. Therefore in high efficient devices a hole limiting layer is used subsequent to the anode electrode.

Generation of singlet and triplet exciton are given Figure 1.8. If parallel spin pairs combine, triplet excitons are formed and if antiparallel spin pairs are combined singlet excitons are formed. Statistically for every three triplets, one singlet is produced due to

electrical excitation. Therefore, the maximum value for η_{st}, ratio of the number of singlets to the total numbers of triplets and singlets, is proposed as 0.25. As mentioned before some researches extend this number to 0.8 and even to 1, and the fraction is not exactly known for each polymer.

Photoluminescence quantum efficiency (η_{pl}) is defined as the percentage of singlets that really emit light. Due to non-radiative decay paths, Figure 1.8, concentration quenching occurs. Not all singlets can emit light and η_{pl} drops. Photoluminescence quantum efficiencies of PPVs are reported as 30 %.

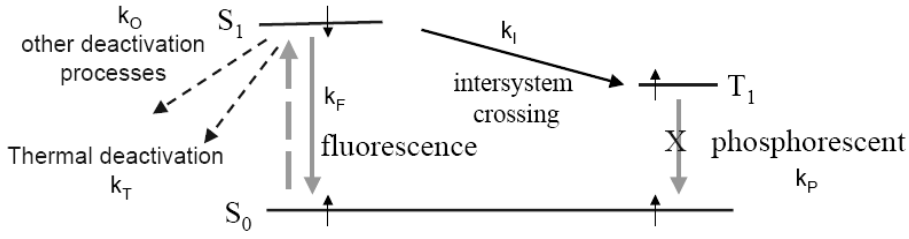

Figure 1.8. Non radiative decay paths shown as k with sub letter, except k_F

1.6. Polymer LED structure

Indium-doped tin oxide (ITO) is normally used as an anode electrode, although other alternatives have also been suggested [66]. It is suitable to inject holes due to its high work function (WF) of about 4.5 eV. Although, the work function of the ITO depends on the deposition conditions [67], its WF can also be enlarged by increasing oxygen content. Polyaniline (PANI) can also be used as a transparent anode electrode. [68] PANI can be deposited as an aqueous solution. Platinum (Pt), Zinc oxide (ZnO), copper phthalocyanine (CuPc), N, N'-diphenyl-N, N'-bis (3-methylphenyl)-1,1'-biphenyl-4,4'-diamine (TPD), N, N'-diphenyl-N, N'-bis (1-naphthylphenyl)-1, 1'-biphenyl-4, 4'-diamine (NPB), or commercial PEDOT:PSS might be used as an option for anode material.

Poly (3,4-ethylenedioxythiophene) -poly (styrene sulfonate)] (PEDOT:PSS) is generally used in PLEDs as a hole-transporting (HT) conductive polymer. It is obtained by doping poly (3,4-ethylenedioxythiophene) (PEDOT) with poly (styrene sulfonate) (PSS). Spin coating its aqueous dispersion on ITO stabilizes and increases the WF to ~ 5.0±0.2 eV. This solves the stability and repeatability problems associated with the dependence of ITO's work function on surface treatment methods and physical conditions of its surface. It

is reported that although the oxygen plasma of ITO improve device's performance by one order, using PEDOT:PSS layer improves performance by further as high as three orders of magnitude [69]. Moreover, by applying conductive polymer layer over ITO, the surface is smoothened and life time of the device is increased. Process diagram and structure of general PLED is shown in Figure 1.9.

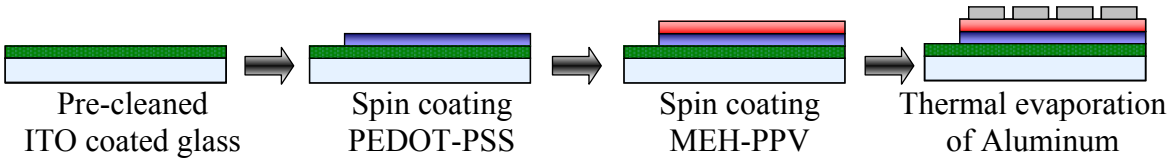

Figure 1.9. Process flow and deposition methods of PLED

Electroluminescent polymer MEH-PPV is soluble in solvents. It is spin coted over HTL. It has a HOMO level at -5.14 eV and a LUMO level at -2.97 eV corresponding to a band gap of 2.17 eV. From electromagnetic radiation equation (1.3), where h is the Plank's constant (6.63×10^{-34} Js) and c is the speed of light (3×10^{8} m/s), λ is the wavelength of light in nm and 1 eV = 1.602×10^{-19} J, the color of light from MEH-PPV is found as orange-red with a wavelength of around ~590nm.

$$E = h\nu = \frac{hc}{\lambda} \tag{1.3}$$

For efficient electron injection, low work-function metal is required to insert electrons into LUMO level of the polymer. Alkali metals like Calcium (Ca), Lithium (Li) and Magnesium (Mg) have the lowest work functions. For example, Ca has work function of 2.87 eV [48] whereas Al has 4.3 eV [3]. However, in the PLED structure Aluminum is used instead of high alkali materials due to high sensitivity of alkali metals to water and oxygen. Alkali metals are easily oxidized at room conditions resulting in the fast degradation of the device. This choice results in an energy barrier (E_b) of 1.33 eV on the cathode side of the junction, Figure 1.10. This big energy barrier to the electrons on the cathode side reduces the number of injected electrons, resulting in a reduction in the device efficiency. However, this reduction in the efficiency can be compensated if the number of injected holes can be decreased to the same level as the injected electrons.

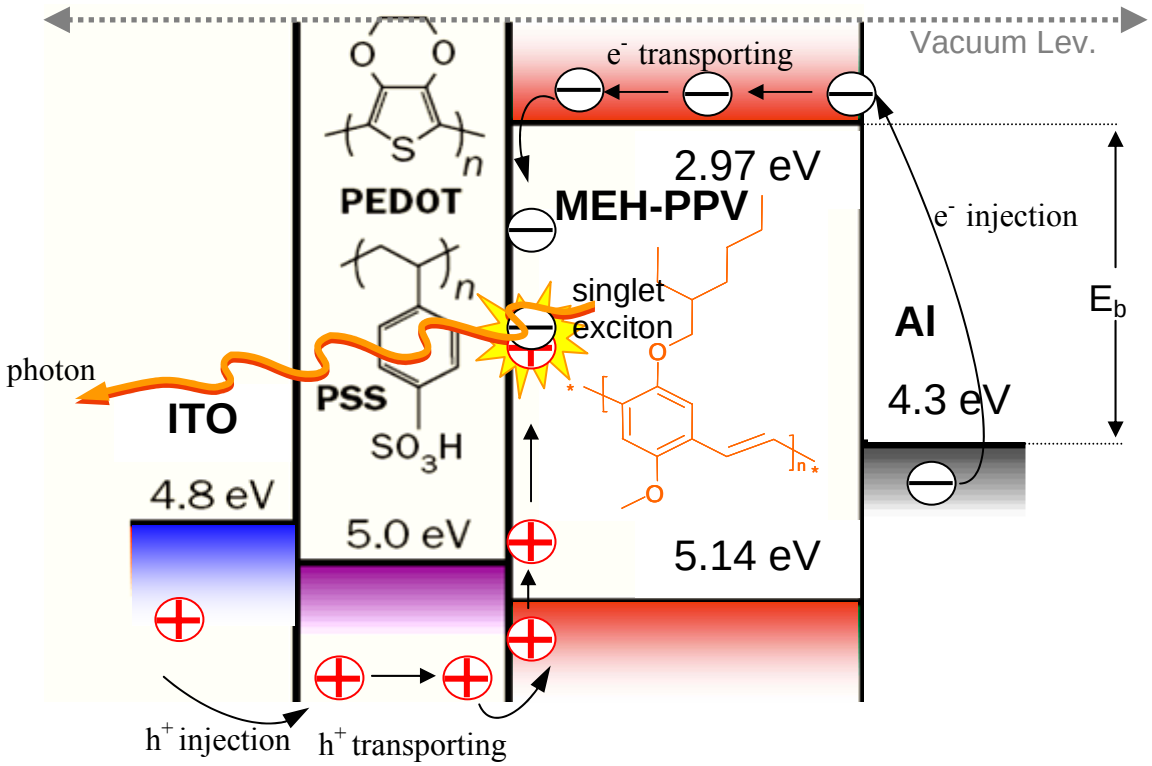

Figure 1.10. Energy band diagram of ITO/PEDOT:PSS/MEH-PPV/Al PLED

1.7. Degradation

Robustness against degradation is the key factor that affects the stability of electroluminescent (EL) device. Degradation not only decreases the performance but also shortens the lifetime of the device.

Formation of dark spots is the common problem in electroluminescent devices. Non emissive small areas are reported to result from delamination of cathode electrode due to heating caused by the pinholes in the metal layer [70]. Some of the areas are short circuited to the electrode on the other side, and some areas become floating due to delamination (Figure 1.11). Also high electric power causes formation of delamination that causes black spots [71]. Black spots also disturb the uniformity of the lighting surface.

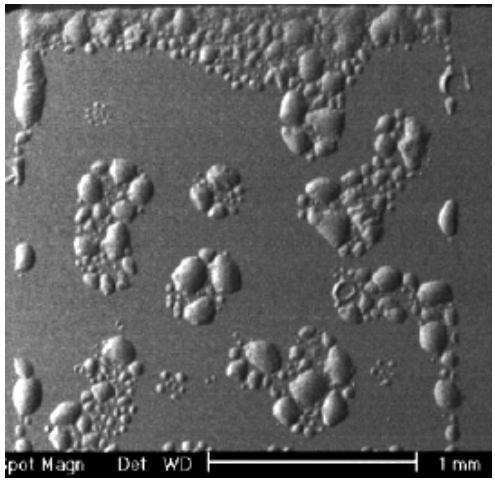

Figure 1.1. Bubble formation [72] on PLED due to delamination of polymers

ITO and polymer interface can also create problems. ITO behaves as an oxygen source and degrades the organic layers. Degraded polymers forms quenching sites. [62]

MEH-PPV is sensitive to photooxidation. During the biasing of the device, length of the polymers enlarges and electron density increases. That makes excited singlet more reactive. Due to longer life time of triplets, singlets decay first and triplets become energetic and transfer their energies to oxygen. This increases non radiative decays.

Devices fabricated in this work are not realized in an inert environment. This is different from other works in the literature. Therefore, the absolute values should not be expected to be compatible with them. This research examines a novel post fabrication treatment method. It compares light emitting and photovoltaic properties of treated and untreated devices that are fabricated under identical conditions. Fabrication details of the samples are given in the subsequent chapter.

2. FABRICATION PROCESS

Conjugated polymers are valuable electroluminescent materials that can be dissolved in numerous solvents and this makes process easier and cheaper. However, organic semiconductors are sensitive to oxygen and humidity. Therefore contamination due to atmospheric gases and chemicals restricts and complicates the fabrication process. However, in our production, all fabrication steps are realized at ordinary room conditions. To understand the effect of the method that we examined, the samples are selected from same wafer with close proximity to eliminate the effects of the variations of fabrication parameters. At the end of the fabrication, electrical and photometric properties of these identical test cells are inspected.

In this part each steps of the fabrication will be presented in detail and the process parameters will be given. The microfabrication techniques such as photolithography, lift-off, spin coating, electrochemical etching, etc. are investigated under the process stages. To achieve repeatable and stable devices all these fabrication process should be characterized and optimum conditions of the process must be determined. Therefore, optimum process conditions and the effects of the process parameters are presented under each production phase. The process steps are given in the Figure 2.1.

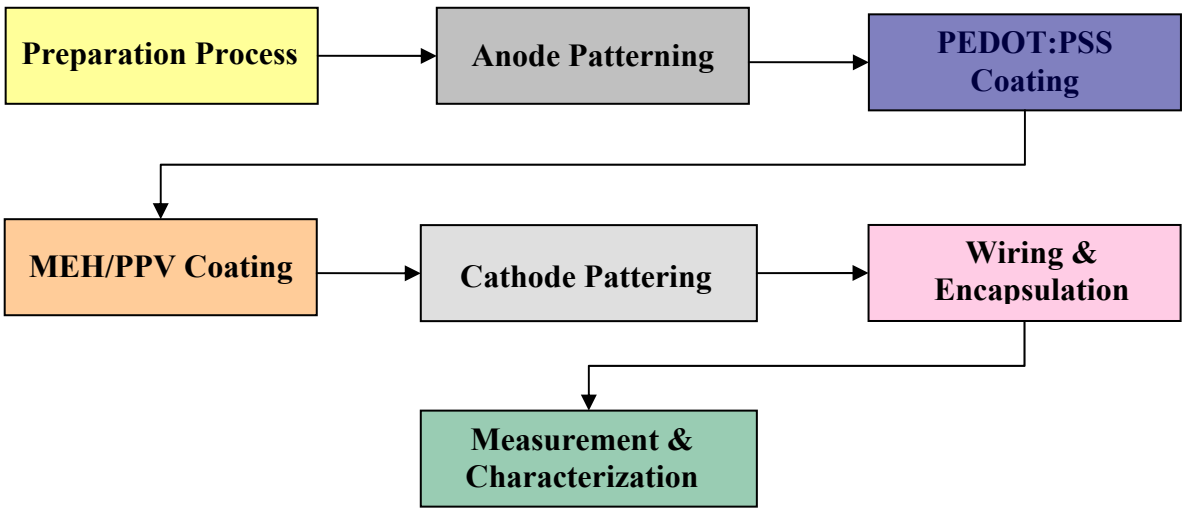

Figure 2.1. Fabrication steps of the polymer light emitting diodes

2.1. Preparation Process

This stage covers the measurements of environmental factors, systematically cleaning the substrates and preparing the required chemicals and apparatuses.

Production in ordinary room environment makes fabrication easier and cheaper relative to the glove box systems because it does not require interconnected glove box systems, special transfer equipments, etc. Fabrication of polymer light emitting diodes is realized at ordinary room conditions with the relative humidity range of 40-50 % and the temperature of 21-26 ˚C. Before the process and during various point of the fabrication, these conditions are periodically measured with multifunctional measurement device (TT-Technic) and tried to control with air conditioner.

As a substrate, 1 mm thick glass wafers are used. ITO coated PET sheets (Aldrich) with a sheet resistivity of 35 ohm/□ are cut into 4” diameter wafer sized circles and attached with silicone gel, shown in Figure 2.2.

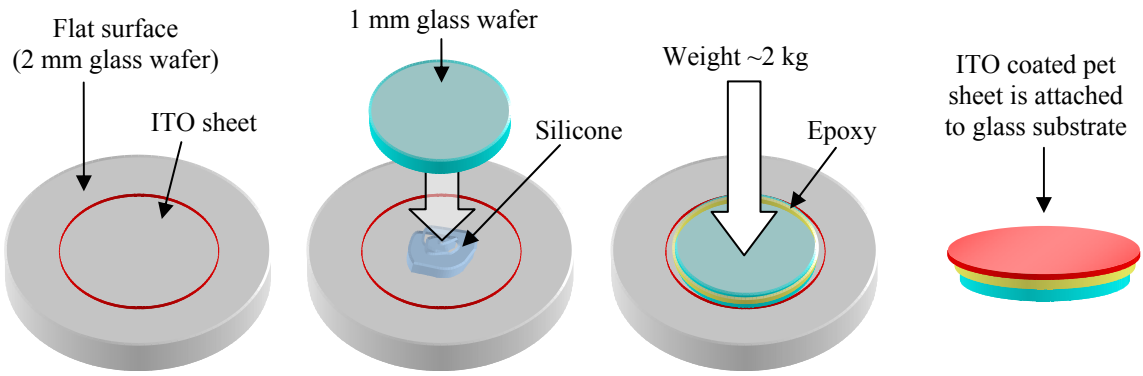

Figure 2.2. The attachment of ITO coated PET to the 1 mm glass substrate

After putting the ITO coated PET sheet to a flat surface, which can be 2 mm thick glass, approximately 2 ml of silicone gel is poured to the pet side of the sheet. Then device is warmed up to 60 ºC on a hot plate, which makes the gel more fluidic. 1 mm glass wafer is placed over the PET sheet and pressed with approximately 2 kg weight, and then the excess of silicone gel is cleaned and small air bubbles are removed out of the gel layer. The force makes silicone layer thinner and assist air bubbles in the gel to leave out of the gel. At the end, the sample is cooled down to the room temperature and excess silicone is cleaned with a piece of cotton soaked in acetone. To prevent the gel trapped between

substrates from escaping and contaminating the cleaning solutions, epoxy glue, Devcon 5 Minute Epoxy, is applied at the contour circle of the wafer, and dried.

Before the fabrication required polymers and other chemicals are to be brought to the room temperature for at least 2 hours before the use. For example, poly [2-methoxy-5-(2'- ethyl-hexyloxy) -1,4-phenylene vinylene] (MEH-PPV) and Poly (3,4-ethylenedioxythiophene) poly (styrenesulfonate) (PEDOT:PSS) must be kept at around 4 °C, so they must be taken out from the refrigerator. That prevents the water condensation on the surface of the bottles. On the other hand, to purify the surface of the ITO from organic and inorganic pollutants, the wafer is cleaned systematically. The protective film on front of the ITO layer must be removed before the cleaning process. Equipments such as bottles, stirrer bars, petri dishes, and tweezers are cleaned with same way. Cleaning procedure covers ultrasonic cleaning of wafer and apparatuses in acetone, isopropyl alcohol and deionized water for three minutes and desiccation of the tools in nitrogen flow.

The structure of the polymer light emitting diode is given in Figure 2.3 and the following fabrication steps describe the required fabrication process.

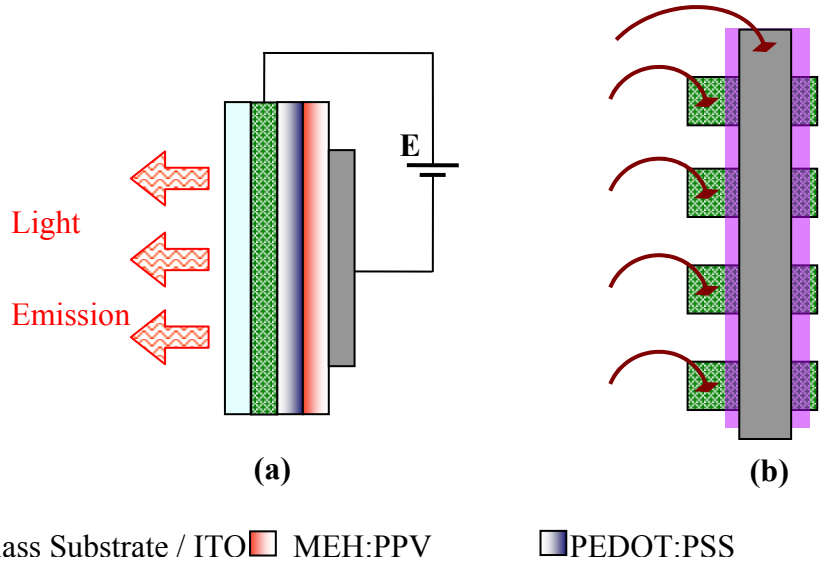

Figure 2.3. (a) Polymer light emitting diode structure and biasing, (b) test cell arrays

2.2. Anode Patterning (Photolithography)

Indium-doped Tin Oxide (ITO) is normally used for the transparent electrode, although other alternatives have also been suggested [72], and due to its relatively high work function it is suitable for display applications. It is normally used to inject holes [73].

The work function of the ITO depends on the proportions in which elements or compounds react with one another and on the deposition properties [74]. Due to lack of equipment resources and standardization capability of the anode material's thickness and stoichiometric properties, ITO sputtered PET sheet are directly bought from Sigma Corporation.

Photolithography, or optical lithography, process is suitable for patterning ITO layer [75]. Latin word photolithography is a compound of words light, stone and writing. Any geometric shapes such as rectangles, circles can be transferred to photosensitive layer coated over the substrate from an already prepared photo mask. Photolithography process is made up of eight steps.

2.3. Preparation of Wafer

After attaching PET sheet to the glass substrate and cleaning procedure, the wafer that holds ITO coated PET is heated to 60 ºC under 0.2 bar vacuum first. That removes water molecules from the surface. To enhance the adhesion of photoresist to the wafer, fast evaporating adhesion promoter hexamethyldisilazane ($[Si(CH_3)_3]_2NH$), shortly HMDS, is spin coated over the ITO surface at 4000 rpm. Adhesion promoters, or primers, deactivate the reactive bonds on the surface and make a polar (electrostatic) shell and enhance adhesion of photoresist (PR), Figure 2.4.

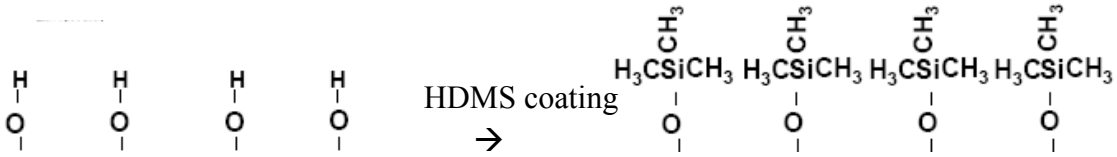

Figure 2.4. Reactive oxygen molecules are deactivated after HDMS coating

Approximately 3 ml of HMDS is dispensed over the wafer and spinned at 4000 rpm. During rotation the waves are observed, called the corona stage. After the formation of the rings is finished that means the wafer is ready to admit photoresist without any interference.

2.3.1. Photoresist Coating

Good adhesion, uniform thickness and thermal stability are the key factors for the selection of photoresist (PR). If the cresol resin molecule chain lengths are small, good

adhesion to the substrate is obtained. Longer chains raise the melting point of the PR. This results in good thermal stability while the surface adhesion gets worse [76].

There are two types of PR; positive and negative. Positive resists dissolved in the developer when they have been exposed, while the unexposed regions stay on the wafer. Negative resists, or image reversal resists, crosslink on exposure and a subsequent baking step, so the unexposed regions of the resist dissolve. Depending on the photo resist type dark field or clear field photolithography masks should be used.

Positive photoresist S1828 [77] from Microchem is used as a photosensitive material for the patterning of the anode layer of the PLED. Not only various thicknesses but also excellent coating uniformity can be obtained between the thicknesses of 2.2–3.2 μm by this photoresist. The spin speed and resulting film thicknesses are given in Figure 2.5. From the figure it is certain that last two digits of PR code give the thickness of layer when it is spin coated at likely 4000 rpm. For our Photoresist Microchem s1828, spin at 4000 rpm, results in 2.8 μm thick polymer layer which is sufficient to protect ITO from etching in target resolution.

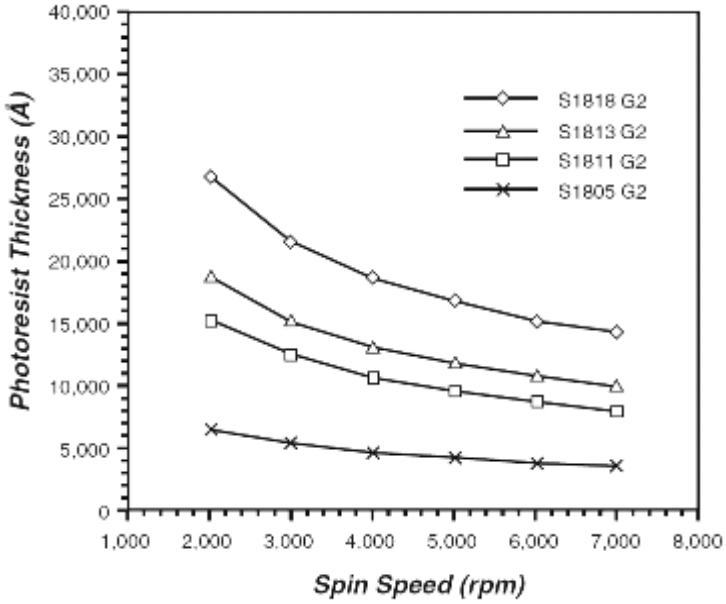

Figure 2.5. Spin speed curves for Microposit 1800 series photoresist [77]

Before spinning PR, it is poured onto the wafer starting from exactly the middle of it without leaving any air bubbles inside. Then the wafer is rotated at lower speeds.

Spreading at w_1 500 rpm for 20 seconds and spinning at w_2 4000 rpm for 30 seconds result in excellent and repeatable photoresist layer. Process speeds are shown in the Figure 2.6.

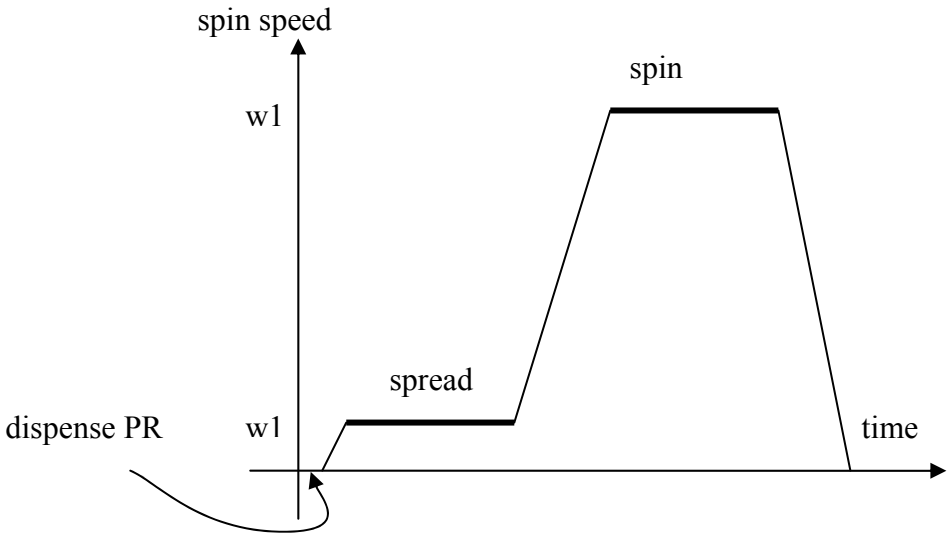

Figure 2.6. Spread and spin speeds for PR deposition

2.3.2. Soft Bake

Solvents in the photoresist should be removed and the top surface of the wafer should be dried before the exposure under UV light source. Therefore, the wafer is placed on top of the hot plate at 90 °C for 1 minute; this process is called pre-bake or soft bake. Period depends on the thickness of PR layer. The temperature and time information are specified in the PR datasheets. If the PR soft bake is not enough, PR layer sticks to the photomask and pollute the mask, because in the contact alignment wafer touches the photomask. On the other hand if the wafer is over soft baked, the development time of the PR layer will significantly increase. Moreover, the thickness of the resist layer is generally decreased by one quarter during soft-bake. [78]

2.3.3. Exposing and Mask Alignment

One of the most important steps in the photolithography process is exposure. The photo-resist coated wafer is exposed through the photo-mask with a high intensity UV light. Generally, a mask is a square glass plate with a patterned opaque layer with high resolution. These high resolution glass photo-masks are expensive. The cost of nanometer fabrication capable mask production facility is about 200-500 million $, and the price of a photomask is varying between 1,000 $ to 100,000 $ [79]. For a typical fabrication process,

approximately from one to twenty photomasks can be used. Because of this prohibitive cost, low resolution PET photomask sheets are preferred in the polymer light emitting diode fabrication to shield photo-resist from photochemical reaction and cost of photo masks is decreased by three orders. Depending on the process, the mask may be aligned to the substrate. By this way, new layer can be deposited relative to the previous patterned layers. For example, the following Figure 2.7, shows the design of anode and cathode layers of the polymer light emitting diode arrays with different sizes. These two masks are used to produce test PLED cell arrays.

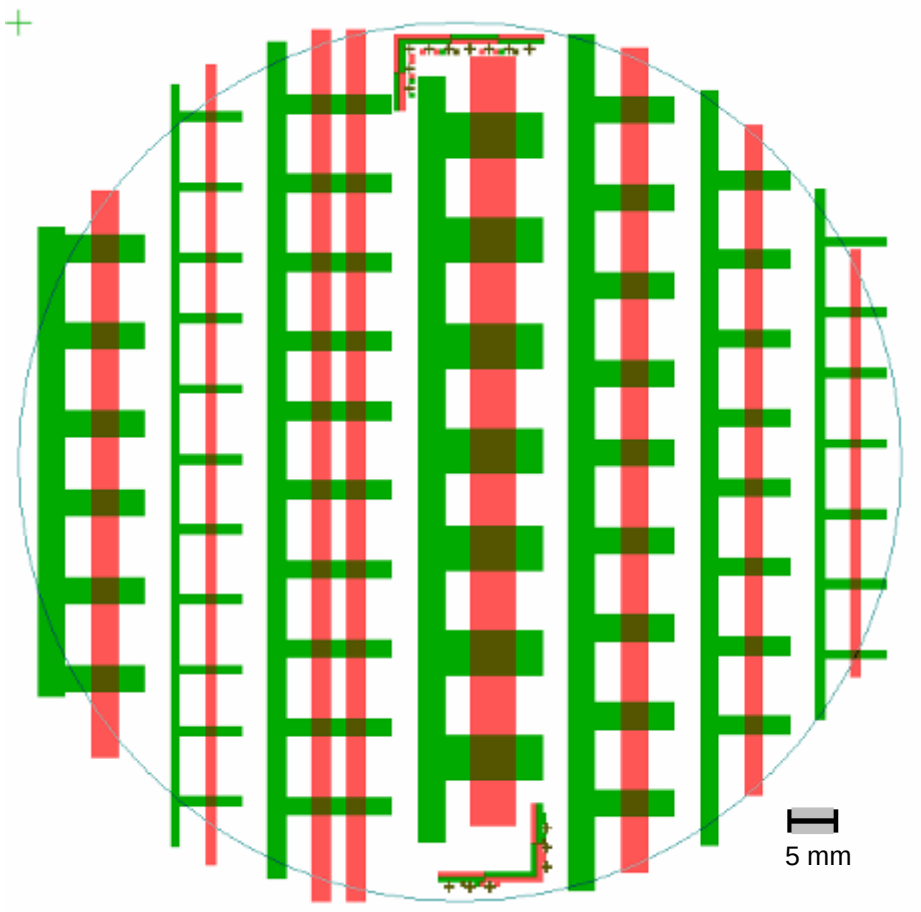

Figure 2.7. The design for two mask fabrication process

In order to align a layer to the previous layer alignment marks are used. The misalignment error can be observed in x, y and θ directions. X and y is the displacement error, θ is the rotational error. To minimize rotational error at least two alignment marks must placed to each layer in distant positions that are as far as possible from each other. Figure 2.8 shows the example of the alignment mark used in the fabrication.

Figure 2.8. Alignment marks for four layer micro fabrication process

Exposure of the photoresist can be realized in three different ways: contact, proximity, and projection [80]. In contact printing, although defects on both resist layer and mask can be formed, due to the physical contact very high resolutions can be achieved. The proximity exposure technique is similar to contact printing but there is 10 to 25 microns space between the wafer and the mask after alignment. This gap reduces mask damage. Projection printing eliminates the damage of mask by the large gap between mask and wafer. The mask image is projected towards the wafer but to achieve high resolution only a small segment of the mask is imaged.

In our polymer microfabrication process, to obtain high resolution and to realize the exposure stage with minimum cost, contact-printing method is selected. To observe the mask and the wafer concurrently for alignment a homemade platform including a microscope and wafer holding stage mounted on micromanipulators is designed. By this way, maximum lithography resolution is observed as 30 µm. If high-resolution glass masks are used in the system, it is estimated that roughly around 5 µm figures can be aligned successfully.

Photoresist 1828 is spin coated over ITO coated film for 30 second at 4000 rpm in previous step. Three minutes and 30 seconds exposure time is enough to expose 2.8 µm thick PR1828 under the custom-made exposure system with the intensity of 5.8 mW/cm^2. The custom-made exposure system is designed in order to minimize the equipment cost. By this way, lithography process is realized that is hundred times cheaper than commercial exposure systems. The system must be turned on at least two minutes before use. At the end of this period the output spectrum of the exposure system reaches the steady state. The steady state spectrum and the custom made exposure system are given in Figure 2.9.

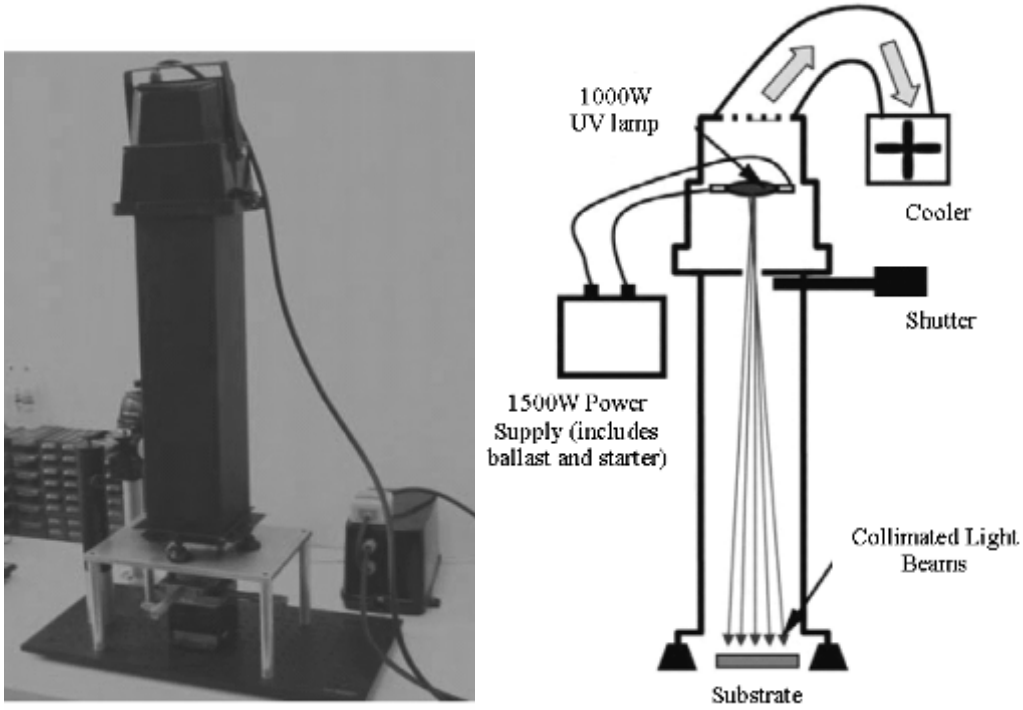

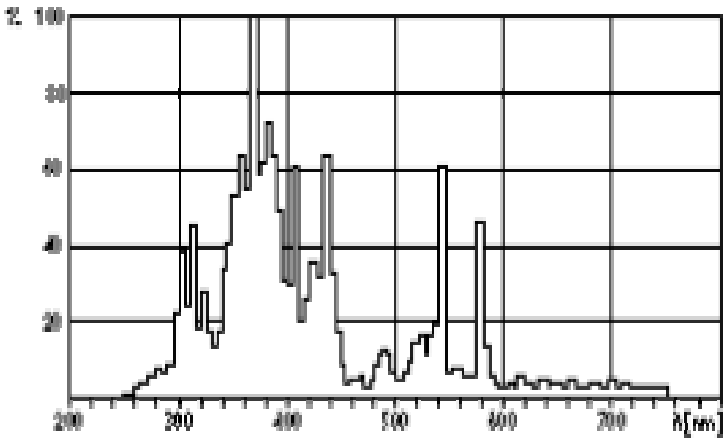

Figure 2.9. Custom-made UV exposure system and output spectrum

The peak wavelength of the custom made exposure system is 380 nm and output intensity is 5.8 mW/cm^2. For high aspect ratios and high resolution transferring, light beams should be perfectly collimated. For polymer display fabrication, light beams with small angles can be acceptable because the figure sizes with dimensions above 30 μm are transferred successfully. For our custom-made system, the maximum beam angle on the substrate is 3.8 ° for the dimensions given in Figure 2.10. If we assume that the gap between the photolithography mask and substrate throughout contact lithography is 0.1 mm at most, the multiplication of the gap length and the tangent of the angle gives the

maximum error occurring on the dimensions of the patterns. The maximum error is calculated as 6.6 μm which is negligible.

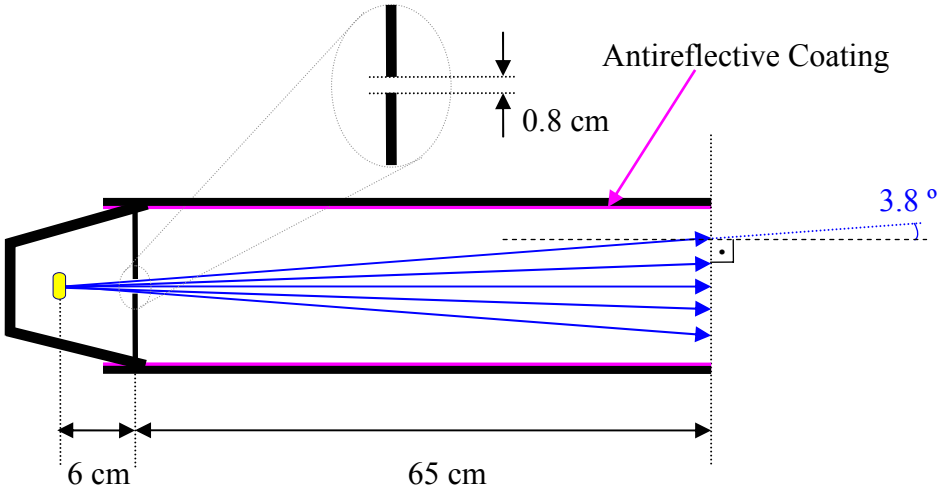

Figure 2.10. The incident angle of the light in the custom-made UV exposure system

If there is more than one layer over the substrate from the Snell' law (2.1), the angle of refraction can be calculated. The law declares the ratio of the sines of the incidence and refraction angles depends on the refractive index of a material, an illustrative figure is given in Figure 2.11. The refractive indexes of some materials are given in Table 2.1.

$$\frac{\sin\theta_1}{\sin\theta_2} = \frac{v_1}{v_2} = \frac{n_2}{n_1} \tag{2.1}$$

Moreover, by the Snell's law the ratio of the velocities of light in two media are equal to the both the ratio of the sines of the incidence / refraction angles and to the ratio of the refractive indexes of two materials.

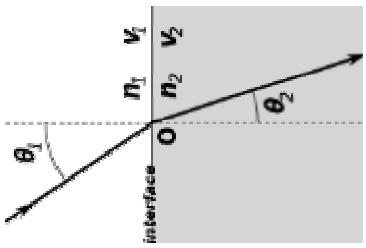

Figure 2.11. Diffraction of a light beam is defined by Snell' law

Table 2.3 Some refractive indices [81, 82] (liquids @ 20 ºC)

Material	n
Vacuum	1 (exactly)
Air (at standard conditions for temperature pressure)	1.0002926
Benzene	1.501
Water	1.333
Ethyl alcohol (ethanol)	1.361
Sodium chloride	1.50
Pyrex (a borosilicate glass)	1.470
Acetone	1.36
Ethanol	1.36
Teflon	1.35 - 1.38
Polycarbonate	1.584 - 1.586
PET	1.57
Glass (impure)	1.485 - 1.755
Fused Quartz	1.46
Silicon	4.01

As a result, to expose photo-resist layer with thickness of 2.8 μm (PR1828), 210 seconds exposure time gives the optimum results. Patterns with dimensions above 30 μm can be transferred successfully by using PET photo-masks.

2.3.4. Development

After exposing the photoresist layer over photomask, the exposed regions become soluble in developer. Developer is a special liquid that allows exposed or unexposed regions of photoresist to dissolve in, depending to the type of photoresist; positive or negative respectively. MF319 (around 3% Tetramethylammonium hydroxide (TMAH) solution) is a developer specified in datasheets for the S1828 type photoresist. Development time is found approximately 45 seconds. Development of the photoresist is realized in a beaker filled with MF319. To stop the process instantly a beaker filled with deionized (DI) water is required. Firstly, photoresist coated wafer is dipped into MF319 filled beaker, and slowly agitated in the vessel. To minimize developer amount used, the

process can be realized in a petri dish with suitable size. On the other hand to accelerate the process, developer may be sprayed over the wafer. At the end of the process, the wafer is quickly washed with fresh developer and sank into DI water beaker. After around two minute agitation in DI water, the wafer is further cleaned with DI water spray and then dried in nitrogen flow.

On a microscope with UV filtered illuminator, the wafer is inspected from different locations if there is undeveloped photoresist residual on the wafer or not. For example, for the positive photoresist 1828 if there is a remaining resist layers on exposed regions, that means wafer is not developed enough and the wafer must be dipped into developer beaker again for 10-15 seconds. The amount of additional time depends on the thickness of the residual photoresist. Similarly, at the end of the additional developing process the wafer is dipped in DI water, dried and inspected again until it is made sure that PR is completely developed.

Generally, at ordinary room conditions (25 ºC) 45 seconds time is enough to develop 2.8 μm thick photoresist by slowly agitating. However, lower temperature decelerates the development process and similarly longer soft bake increase development period.

2.3.5. Hard Bake

To stabilize and solidify the developed photoresist that is patterned in the previous step, hard bake, or post bake, is required. Heating the wafer at higher temperature harden the PR and assist the PR polymer to fill the pinholes on the layer. The heating process can be realized on hot plate, shown in Figure 2.12. In our process, PR layer of S1828 with thickness of 2.8 μm is hard baked at 110 °C for 30 minutes. If the wafer is hard baked longer or the temperature of the process is higher, the removal, or stripping, of resist layer will be more difficult. Post-bake is not needed for processes in which a soft resist is desired, e.g. metal liftoff patterning.

Figure 2.12. After developing the photoresist, the wafer is hard baked at 110°C on hot plate

2.3.6. Etching

PR coated and hard-baked samples are etched in Hydrochloric acid ($HCl:H_2O$) (1:1) for 45 seconds. ITO reacts with HCl and isotropic ally etches the ITO layer with thickness of 1200 ºA. Etch rate at 26 ºC is 2.6 nm/s. Lower temperature decelerates the etch speed since reaction slows down. For example, in our trials at 18-20 ºC the etching process takes about three minutes. Process takes place in a beaker filled with 250 ml HCl and 250 ml DI water, and to stop the reaction high volume of beaker filled with DI water is prepared near the etchant solution.

The etch rate is relatively slow as compared to target figure sizes, process resolution, of the fabrication. Our fabrication aims the production of figure sizes above 30 µm, therefore 1 µm undercut is acceptable in etching process. Thus, the etch duration is not significant because etch rate is too slow as compared to figure sizes. For example, if the wafer is left for five minutes in addition to compulsory 45 seconds in the etchant solution, at most 1 µm undercut will be observed which is tolerable.

Moreover to accelerate the process different methods can be tried. For example, the content of the HCl in etchant solution might be increased. $HCl:H_2O$ (4:1) solution can achieve the etch rate of 50 nm/s [83]. On the other hand, heating the solution also accelerates the chemical reaction, so decreases the process time required. But, the temperature increment is not an effective solution, because it extends the process time.

Adding hydrogen fluoride (HF) to the solution (1:1:10) ($HF:H_2O_2:H_2O$) increases the rate six times compared to the hydrochloric acid. [84]

As a result, figures with resolution above 30 μm is successfully transferred to ITO layer, shown in Figure 2.13.

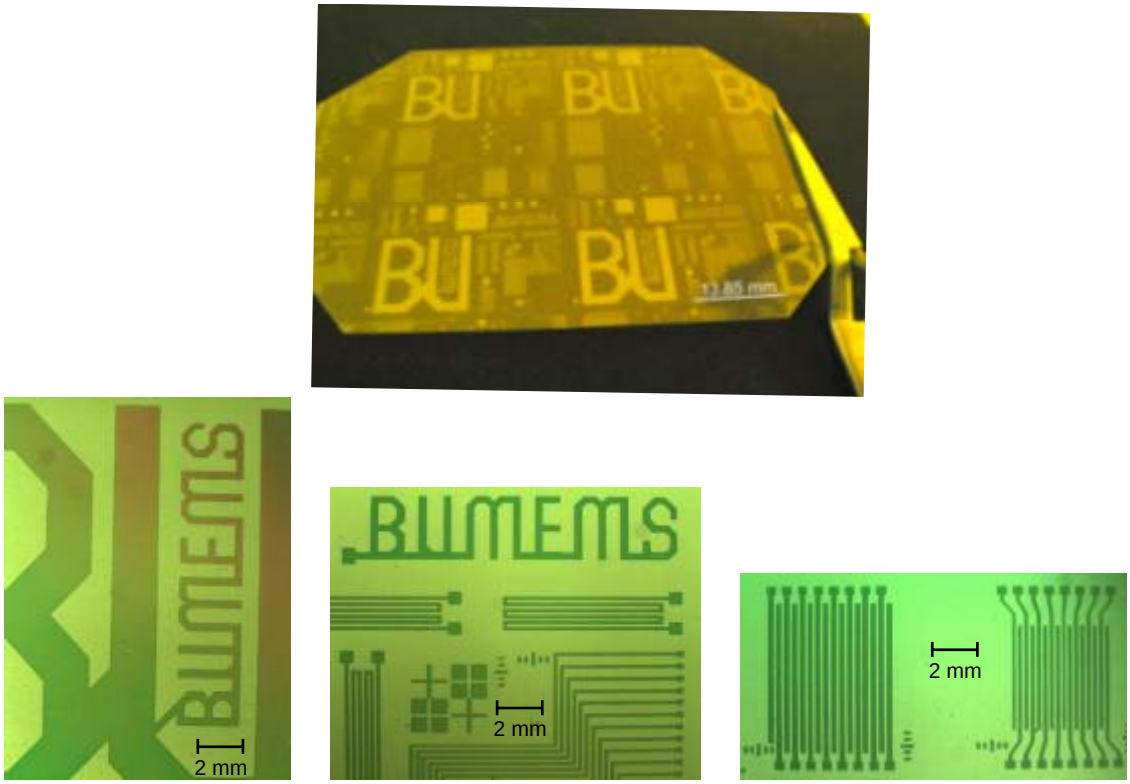

Figure 2.13. Patterned ITO wafer and figures obtained

2.3.7. Stripping

After etching the ITO layer, PR film is stripped in solvents until completely removed. Ultrasonic cleaning method might be more effective. Standard cleaning procedure is applied to the wafer after roughly washed in small acetone spray. The wafer is ultrasonically cleaned in acetone, isopropyl alcohol (IPA) and DI water successively each for three minutes. Then, wafer is dried in nitrogen flow. Depending on the hard baking process time and temperature, some PR residuals may be observed on the wafer after the stripping process. In this case, the repetition of the cleaning procedure is required.

On the other hand, oxygen plasma ash might be used for the removal of organic materials. Since we do not have high power plasma machine in our facility, first photo

resist is striped with wet solvents, then to remove small polymer dusts, low power oxygen plasma is applied to the wafer.

2.4. Hole Transporting Layer Deposition

PEDOT:PSS, or Poly (3,4-ethylenedioxythiophene) and poly(styrenesulfonate), is a conductive polymer, which is mixture of sodium polystyrene sulfonate and sulfonated polystyrene, used as a hole transport layer. Moreover, the surface of the ITO layer is rough and causes local short circuits when the device is biased. The presence of PEDOTPSS layer smoothens the irregular surface of ITO and improves the performance the device. Additionally, PEDOT-PSS layer acts as a barrier between ITO and electroluminescent polymer and blocks the oxygen and iodine atoms to diffuse to the light emitting polymer layer. Furthermore, it has a repeatable work function value unlike ITO. This is significant for the stability, repeatability and lifetime of the device.

The solution of PEDOT:PSS is bought directly from Sigma as an aqueous dispersion. Hole transport layer, PEDOT:PSS is deposited over patterned ITO film with spin casting method. Due to the hydrophobic nature of the surface, polymer solution can not be spin coated directly. High viscous surfactant, Triton x-100, is added to the PEDOT:PSS to eliminate hydrophobic character. For 4 inch wafer, (1:1000) (Triton x-100) : (PEDOT:PSS) solution is prepared with 5 ml PEDOT:PSS and 5µl Triton x-100. The blend is stirred with magnetic bar for 10 minutes. Then the solution is filtered with Teflon syringe filter, Anotop 0.2 µm, which has a glass microfibre prefilter.

On the other hand, to eliminate the hydrophobic nature of aqueous dispersion of PEDOT:PSS (Sigma) on PET surface, oxygen plasma with a power of 1.3 W is applied for 15 minutes under 300 mTorr vacuum. This enhances the adhesion of PEDOT:PSS polymer and purifies the surface of the ITO from organic pollutants.

Approximately 100 nm thickness of PEDOT:PSS film is obtained by spin coating technique. First, solution is spread for 10 seconds at 200 rpm and then spun for 30 second at 1200 rpm. On coating, samples are dried for 30 minutes at 110 °C hot plate. After 30 minutes period, to remove water and oxygen as much as possible, first the sample is put on the hot plate, second it is closed with desiccators cap and filled with nitrogen. Then the sample is vacuum baked at 110 °C under 0.2 Barr for additional one hour. The hard bake

process increases the conductivity of the PEDOT:PSS film and removes the solvent (water) in the polymer. Moreover, the temperature is increased and decreased smoothly to minimize the surface tension.

2.5. Electroluminescent Polymer Deposition

To dissolve the MEH:PPV in toluene, 16 mg MEH:PPV is poured into 4 ml toluene solution and stirred on hot plate at 50 C°. The mixture should be stirred at least 4 hours until the polymer is fully dissolved. The solution is prepared in dark glass (10 ml) bottle to prevent light diffusion. The bottle is covered with aluminum sheet to heat the solution more uniformly and to guarantee the blocking of light .

After cooling down the solution to room temperature, the mixture is filtered with Teflon syringe filter (0.25 μm). MEH:PPV solution in toluene is spin coated at 2000 rpm to obtain the film thickness of approximately 80 nm. At the end, polymer film is baked at 65 C° for one hour on hot plate.

With decreasing film thickness; luminous efficiency of the light emitting device increases and the dominant wave length decreases [85], shown in Figure 2.14. Therefore, the test cells are selected from the same wafer. Otherwise, their electrical and photoluminescence characteristics might be completely different.

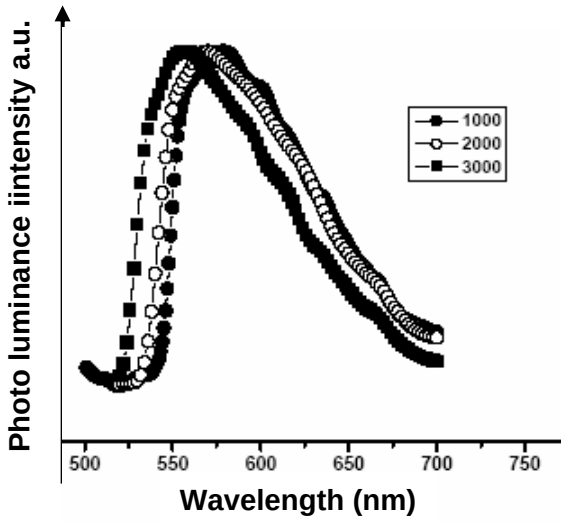

Figure 2.14. Patterned ITO wafer and figures obtained [14]

2.6. Cathode Deposition

While the positive electrode has a high work function so that it can supply holes or attracts electrons from the polymer, the negative electrode must be selected to have a low work function so that electrons can be easily injected. Ca, Mg, Lt and Al have low work function so suitable for the cathode electrode.

Thermal evaporation is a universal method for thin film deposition. In high vacuum environment source material is heated and evaporating particles freely depart from the source and travel straightly towards the target. The system components of the thermal evaporator are shown in Figure 2.15. Due to vacuum and kinetic energy of the hot material, vapor molecules freely moves and escape from the source boat.

Aluminum is deposited as a cathode electrode. Approximately 400-500 mg aluminum source material is cut into pieces and cleaned systematically in ultrasonic bath. Then metal pieces are dried with dust-free wipe, and slow nitrogen flow. The amount of source material depends on the target thickness of the film.

After the wafer is mounted onto the target wafer position and the source material is loaded, the vacuum level of the evaporator is decreased by mechanical pump to $3x10^{-2}$ Torr, then the system automatically runs the diffusion pump. Around 6-8 hours after turning on the diffusion pump, the vacuum level reaches $5x10^{-6}$ Torr. On satisfying the required vacuum, filament and crystal cooling system, main power units are turned on. On the thickness monitor device, right material must be selected before the evaporation. The power transmitted to the tungsten filament is increased slowly until the evaporation starts. On starting the evaporation, shutter that prevents uncontrolled deposition is opened and deposition rate is manually fixed at 4-8 Angstrom/second. When the target thickness is reached shutter must be closed and power must be decreased slowly and turned off. At the end, the vacuum is vented to room pressure and system is turned-off.

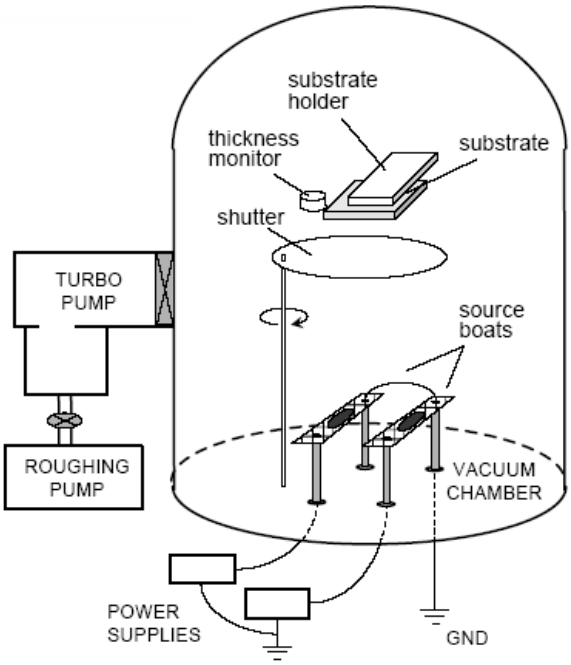

Figure 2.15. The system components of the thermal evaporator

Cathode layer, aluminum, is patterned with two methods; shadow mask and lithography. The fabricated PLED devices with these methods are shown in Figure 2.16. Shadow masking is safer because the fabricated PLED does not get in contact with wet chemicals so it does not get contaminated. But, the masking material is very important. The masking material must not out-gas in high vacuum at high temperatures like 80–100 C° because it will be used under high vacuum in evaporator chamber.

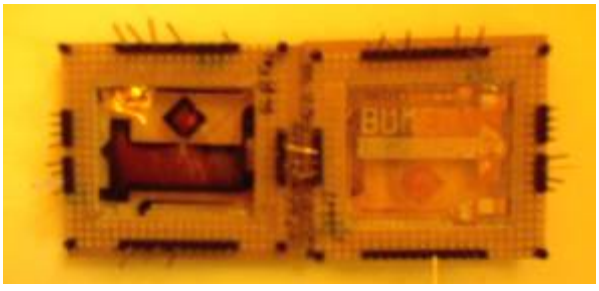

Figure 2.16. Aluminum layer is patterned with shadow mask (left), wet etching (right)

2.6.1. Pattering of Cathode Layers with Shadow Mask

To prepare a shadow mask, or shielding film, two methods can be used; dry and wet etching. Wet etching means removal of desired regions of the shielding depending on the design in liquid etchant. Especially, conductive shielding materials, or metals, are highly

suitable for this method and they do no out-gas in vacuum. Dry etching of the shielding film can be realized by a laser cutter. This is less time consuming process and good for prototype fabrication.

2.6.1.1. Shadow Mask Preparation with Wet Etching The ideal shadow mask material must be very stiff, thin and a non-out-gassing material. Metal films successfully solve this problem and wet etching is suitable for metal engraving. Although there are disadvantages like undercutting, see Figure 2.17, and rounding of the sharp corners, see Figure 2.18, the isotropic etching is an easy and simple method which is the best for large geometries.

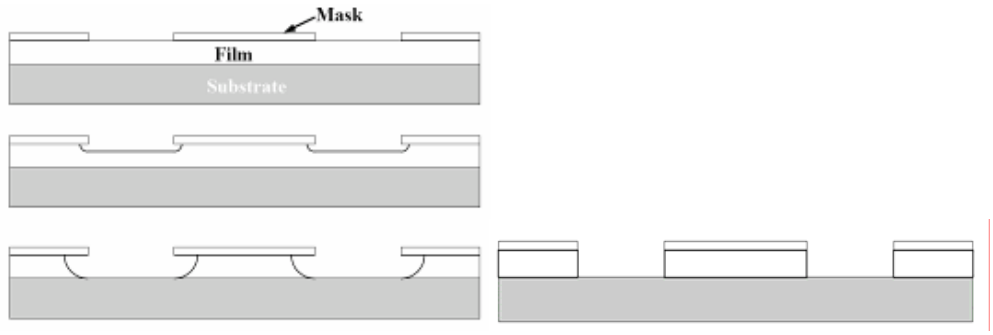

Figure 2.17. Isotropic vs. Anisotropic Etching

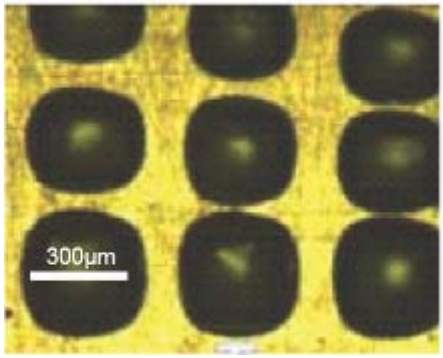

Figure 2.18. Isotropic etching results in rounded corners

2.6.1.1.1. Mask Patterning with Wet Etchant Wet etching is the simplest and the easiest method for engravement. The only restriction is that mask material and etchant must be suitable to the application. In other terms etchant must be selective to masking material. As compared to the dry etching in microfabrication, wet etching is 1-2 orders of magnitude cheaper than dry etching. [86] To obtain higher resolution really thin shielding materials should be used, since undercutting will be equal or grater than the material thickness. For etching metals, the following wet etchant, shown in Table 2.2, can be used.

Table 2.4 Wet etchants for some metals

Metal	Etchant
Copper and Nickel	30 % $FeCl_3$ 5 % Piranha (30 % H_20_2:70 % H_2SO_4) KI:I_2:H_20 (Not transparent)
Chromium- (requires depassivation)	Aqua Regia (75 % HCl: 25 % HNO_3) HCl: Glycerin
Gold (Au)	Aqua Regia Iodine Alkali Cyanide w/Hydrogen Peroxide
Silver (Ag)	Iodine HNO_3

For our fabrication, to prepare a shadow mask with thickness of 50 μm stainless steel type 304 [16] or copper film can be used. As a shielding material, thick PR layer is used. That can be obtained by spin coating of S1828 photoresist at 2000 rpm over finely polished metal surface. Rough metal surface really disturbs the etching process and creates pinholes on the shadow mask. Therefore, metal surface must be cleaned, or polished, with the finest sandpaper. The final cleaning can be made with wet sand paper; this reduces scratches and polishes the surface.

2.6.1.1.2. Mask Patterning with Electrochemical Etching For deposition of shaped aluminum films, using shadow mask can considered as the simplest and the safest technique. As said before metals do not release intrinsic gases in vacuum. One advanced type of wet etching is electrochemical etching. It is faster than wet etching and appropriate for metals because they are electrically conductive. Principle set-up for the electrochemical etching process is shown in Figure 2.19.

In electrochemical etching, electric field is applied to two electrodes of which one is to be etched and other collects ionized particles. Throughout process, metal releases free electrons to solution by ionizing and opposing electrode accepts electrons resulting in chemical reactions. For example, depending on the metal such ions like copper (Cu++), Al+++, sodium (Na+) , potassium (K+), Ca++, Mg++, zinc (Zn++) , chrome (Cr++) ,

cadmium (Cd++), titanium (Ti+) , nickel (Ni++) , lead (Pb++) , iron (Fe+++) , H+, arsenic (As+++) , Li+ , Ag+ , quicksilver (Hg++) , Au+++ , Pt+++ are formed in the electrolyte. Electrochemical etching, EC, could be thought as forced corrosion. Etching time changes from several seconds to couple of hours. The process is dependent on current density, temperature, pH of the electrolyte and the concentration of the electrolyte. Due to isotropic manner of etching, the thickness of metal film must be as thin as possible. Also shadow mask film must be feasible to mount in front of wafer and durable during the evaporation process. Because of the commercial availability, copper film with thickness of 0.05 mm is selected as shadow mask material.

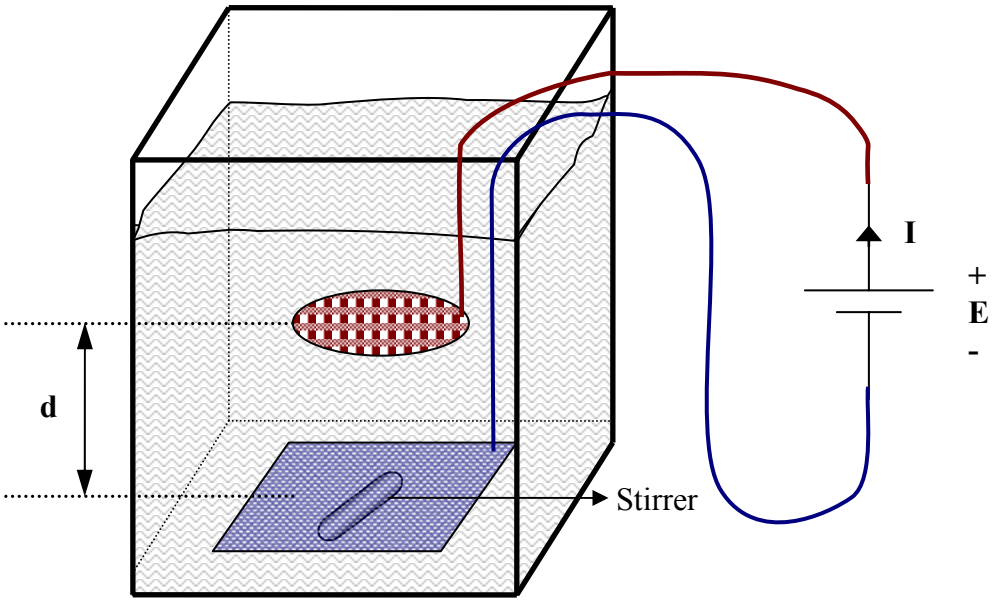

Figure 2.19. Electrochemical etching principle

In our process, we design a custom-made platform, Figure 2.20, for EC etching. This stage assists us to keep the distance between electrodes constant and to fix the electrodes parallel to each other, shown in the photograph below. Also, the distance between the electrodes is adjustable.

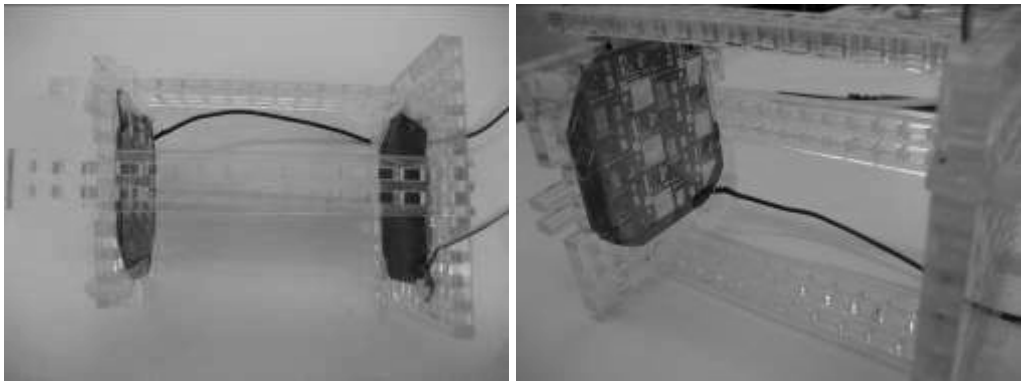

Figure 2.20. Custom-made electrochemical etching stage

Table 2.5 Electrochemical etching experiments and results

E (V)	I (A) start/stop	d (mm)	Stirrer	Duration (min)	Results for the solution for EC etching is ($HCl:H_2O$) (1:1)
5	0.2 0.03	7	ON	37	Minimum 0.08 mm gap between holes is required, unless they combine. The roughness of the metal surface is the crucial factor determining resolution.
10	0.25 0.05	25	OFF	35	Stirring decreases the sharpness. Increment in the voltage accelerates the process.
13	2 0.04	2	OFF	7	Only rough figures can be obtained. Although this is the fastest process, figures with size of below 1 mm are mostly damaged.
5	0.3 0.03	25	OFF	40	Good for the figure with size of 100 μm, and 100 μm spacing is required.
3	0.22 0.05	25	OFF	50	To obtain finer figures, voltage decreased and surface of the metal is polished with sand paper.

The most crucial factor for shadow mask preparation with electrochemical etching is the surface roughness and the purity of the material. The results of the electrochemical etching are summarized in Table 2.3. The resulting test patterns are shown in Figure 2.21.

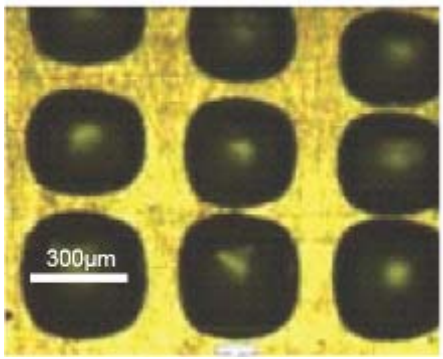

Figure 2.21. Shadow mask prepared by electrochemical etching

To obtain smaller patterns, thinner films must be preferred since the process is isotropic. For example to obtain a line with 10µm width, the thickness of the metal film must at least 5 µm. Moreover, the process duration obviously depends on the current passing through the cross sectional area of the open field on the metal film. At the end of EC etching trials, shown in the Table 3, for 50 µm copper film; under electric field built by applying 3 V to electrodes separated by 25 mm, although 50 µm size can be obtained fairly, to guarantee the results minimum 100 µm patterns with 100 µm spacing is proposed for the mask design.

Aluminum cathode layer is patterned by a copper shadow mask prepared by EC etching similar to the one shown in Figure 2.22. This step finishes the fabrication of the polymer light emitting diodes as shown in Figure 2.23. After the metal deposition, PET substrate holding the fabricated devices is detached from the glass substrate.

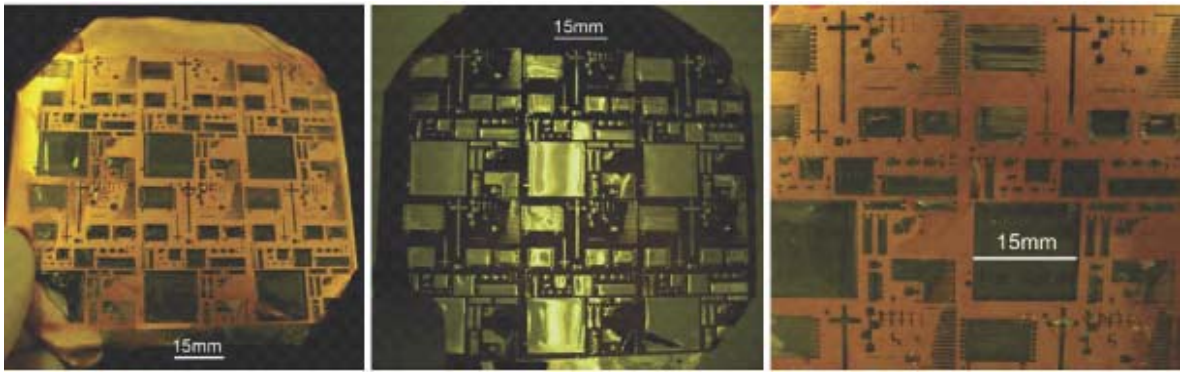

Figure 2.22. Etched copper film mounted on glass substrate

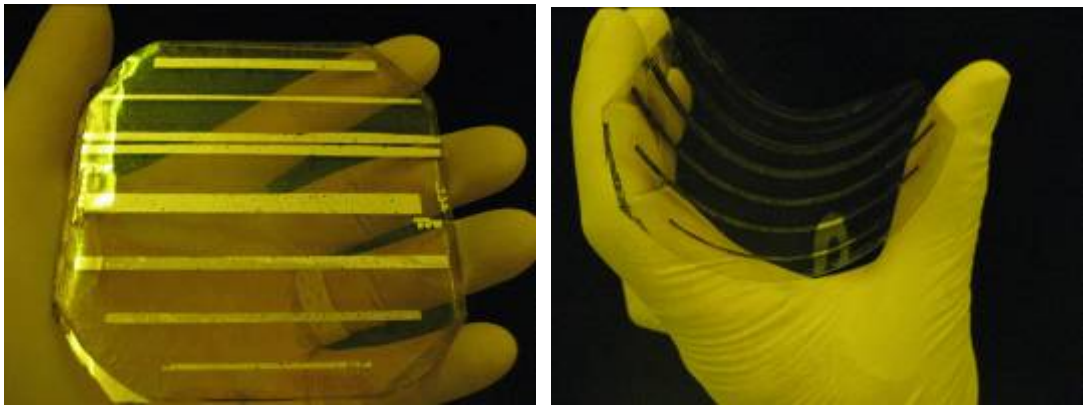

Figure 2.23. PLED with aluminum layer that is patterned with copper shadow mask

2.6.1.2. Shadow Mask Preparation with Dry Etching In microfabrication, dry etching such as plasma etching (plasma-assisted chemical reaction) and reactive ion etching (RIE) (chemical reaction and ion bombardment) high resolutions can be obtained. But these systems are really expensive and designed for high resolution microfabrication. However, our process did not need this resolution. Therefore, an industrial manufacturing process, laser cutting, is used. This method is widely used for prototyping and small lot fabrication.

Plexiglas, (fire resist) FR4, or regular paper sheets can be micromachined in laser cutters. The cost of fabrication is 1-3 orders of magnitude cheaper than dry etching methods used in microfabrication.

Computer aided design (CAD) drawings can be transferred to mask material in couple of minutes. For example, making the shadow mask from paper with the CAD drawing given in Figure 2.24 takes about 30 minutes. Process time mostly depends on the length of contour lines.

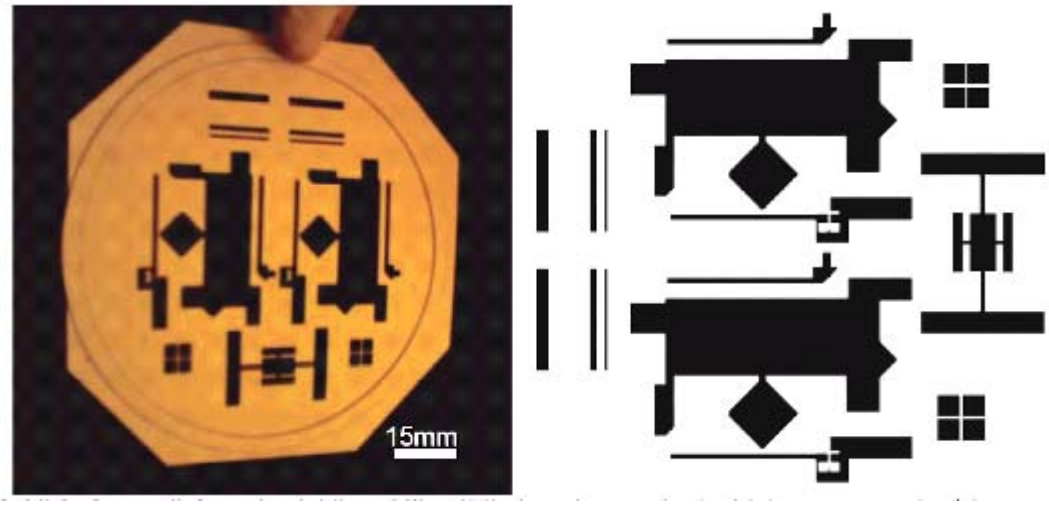

Figure 2.24. Shadow mask prepared by laser cutter (left) and its CAD design (right)

However, shadow masks prepared from paper or polymers like Plexiglas could not be used in PLED fabrication because they out-gas during thermal evaporation. They pollute deposition and disturb the shape of the figures, shown in Figure 2.25. Therefore, materials that can be processed in laser machine but that do not release gas in vacuum must be preferred for the preparation of shadow mask in laser cutter. For the Versa Laser Cutter VL 200, the speed of 5, pulse per inch (PPI) of 1000, power of 100, line weight of 0.015 mm, Z distance of 1mm is a good starting point for patterning FR 4 with thickness of one millimeter. Depending on the results power, speed, PPI parameters can be varied. In laser cutter, patterns of 300 μm can be obtained over 100 g / m^2 paper.

Figure 2.25. Effect of out gas from the shadow mask on thermally evaporated film

Moreover, materials like metals, teflon, polyamide and glass can not be processed in laser cutter.

2.6.2. Pattering of Cathode Layer with Lithography Process

2.6.2.1. Cathode Pattering with Wet Etching Process Wet etching of cathode electrode aluminum is same as the pattering of ITO layer. MF 319 which is developer for S1828 photoresist etches the Al layer. The main asset of MF 319 is that it is selective to ITO, and polymers. After aluminum deposition in thermal evaporator, photoresist layer is applied, soft baked, exposed and developed. To etch the metal layer developing process extended from 45 second to 10 minutes. Since MF 319 is really selective to photoresist, Aluminum layer is patterned without problem. Different from the ITO patterning, to stop the developing or Al etching, wafer must not be dipped into DI water. Water dissolves PEDOT:PSS layer and lift-off the layers above (MEH-PPV and Al) as shown in Figure 2.26. Therefore, to clean MF 319 isopropyl alcohol (IPA) is sprayed over the wafer. And to strip photoresist acetone is sprayed to the wafer. Then wafer is dried in nitrogen flow.

Figure 2.26. Water lifts-off PEDOT:PSS and the coatings above it

By wet etching 120 nm Al layer, 50 μm resolution is obtained successfully, as shown in Figure 2.27. By this method not only Al layers, other metal layers can be patterned.

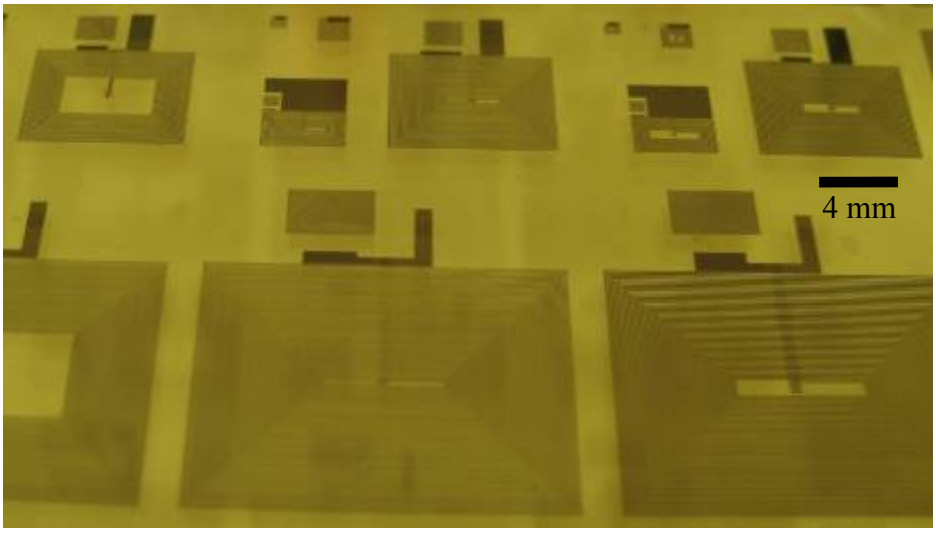

Figure 2.27. Thick aluminum (120 nm) layer patterned by wet etching

2.6.2.2. Lift-off process Although lift-off process is not used in this work to pattern cathode layer of the PLED, the method is used for making metallic patterns on any substrate, especially for those noble metal thin films such as platinum, tantalum, nickel or iron which are difficult to be etched by conventional methods. In single layer lift-off process initially a pattern is defined on a substrate using sacrificial layer like photoresist. A metallic film is deposited over the wafer. This covers the photoresist and blank regions. Then the photoresist under the film is removed with suitable solvent, which removes all the layers deposited on the photoresist.

One of the crucial factors in lift-off is that during thermal evaporation, temperature of the wafer should not exceed the soft bake temperature. Otherwise, it may burn the photoresist and the PR layer can never be cleaned. Second issue is that the adhesion of the deposited film on the substrate must be excellent, if not all deposited layer might be removed during the photoresist removal. Moreover, thicker deposited layers prevent the photoresist from being wetted by the solvent; therefore, the deposited film must be thin and has a grainy surface. [88] As a result, to prevent burning of PR, wafer is mounted on a metal bulk substrate with thermally conductive glue and aluminum tapes. Furthermore, the Al layer is deposited not too thick, as shown in Figure 2.28.

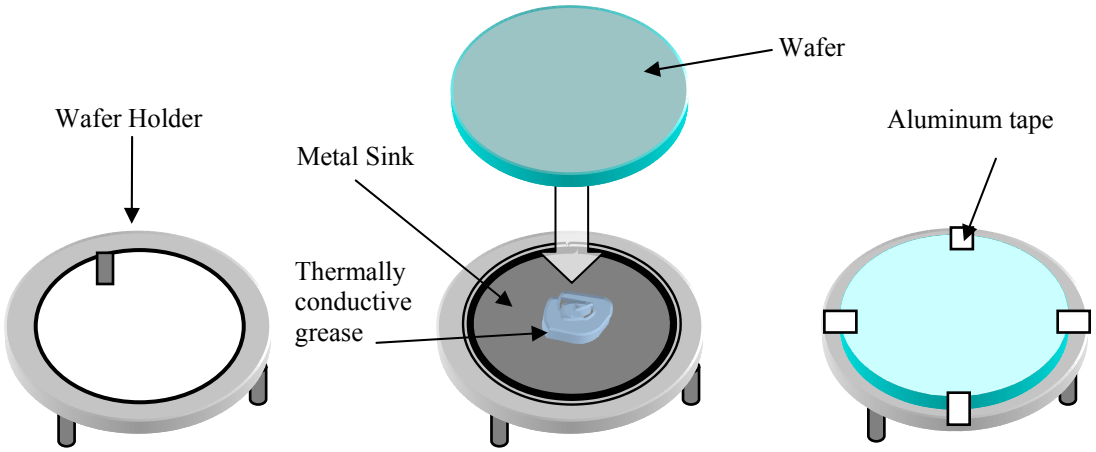

Figure 2.28. The attachment of wafer to the wafer holder of thermal evaporator

In our experiment we observed that elasticity of the deposited material prevents the removal of the layers and disturbs the edges. For instance, lifting-off a gold layer is more difficult than chromium or aluminum. Therefore, the deposited material should be brittle.

On the other hand, creating an undercut profile is another key issue in lift-off [89]. Soft bake temperature, soft bake time, exposure intensity and time and development time influence the slope of the resist walls. To provide undercut profile, wafer is soaked in cholorobenzene after the exposure [90]. This hardens the surface of the photoresist and decelerates the development rate of the outer shell. Moreover, the thickness is increased in some ratio by this way.

For the successful lift-off process with S1828 photoresist, standard photolithography procedure is experienced with 1000 rpm spin speed and 10 minutes of soft bake at 90 ºC. Process flow and layers are shown in Figure 2.29. After 210 seconds of exposure, the wafer is soaked in cholorobenzene for 5 minutes. A suitable sized Petri-dish can be used for cholorobenzene bath. Under developing photoresist is really risky since PR residuals left on the wafer causes evaporated metal not to stick on the wafer surface, and results in complete removal during PR stripping. Therefore, PR is developed in MF 319 with agitation for 5 minutes. At the end of the development wafer is washed in DI water for 2 minutes and dried in nitrogen. After the deposition of the metal layer, photoresist layer can be removed by dipping in acetone. The duration of lift-off time depends on the film thickness, film quality (higher quality, longer lift-off), the temperature of deposition, and type of the solvent. For the lift-off process described above, 5 minute acetone bath is

enough to remove PR layer. Residual metal layers, especially on sidewalls, may be cleaned with small swipe of a cotton swab or spraying acetone to the wafer may be tried. The substrate is dipped in acetone until all the film has been lifted-off. Generally, for the process conditions described above, 80 % of the layer is removed in the first 5 minutes period. Moreover, once a metal particle dries on the substrate, it is difficult or impossible to remove it, therefore the wafer must not be taken from acetone solution or dried until it is made sure that lift-off is finished.

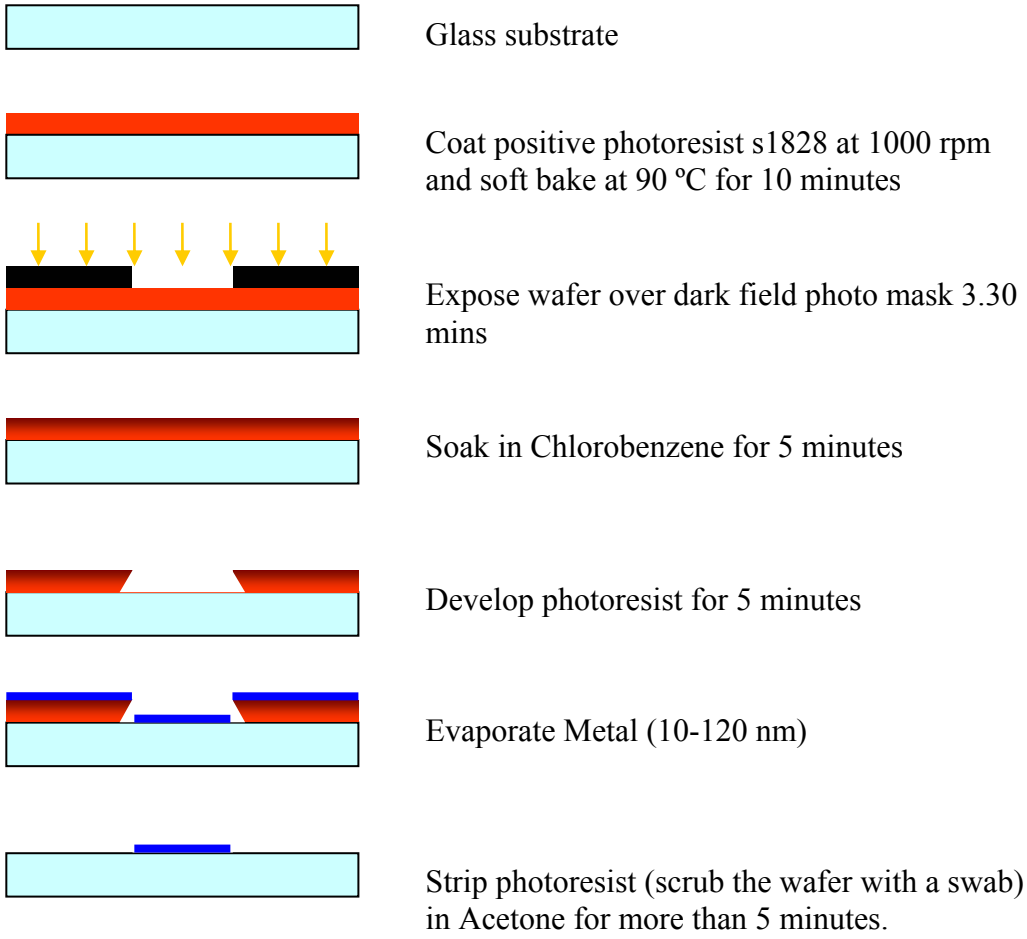

Figure 2.29. Steps of single layer lift-off process

2.7. Packaging and Wiring

After aluminum deposition, samples are cut and attached to a thin glass substrate to prevent oxygen and water diffusion from their PET sides and wired. Then, PLED arrays are thermally and electrically treated on hot plate. Treatment process will be given in detail

in the next chapter. After wiring and treatment procedures, the samples are encapsulated with hot melt silicon grease, shown in Figure 2.30, purchased from Bayer. The thick silicon layer is a good barrier for moisture and oxygen.

Figure 2.30. Wired and encapsulated PLED samples

For the demonstration of the light emitting diodes, the packaged samples are attached over FR4 frames. These frames include socket connections, as shown in Figure 2.31. By this connection, junctions can be biased and manipulated by electronic driving circuit. A driving electronic circuit is designed and implemented to test these packaged PLEDs as explained next.

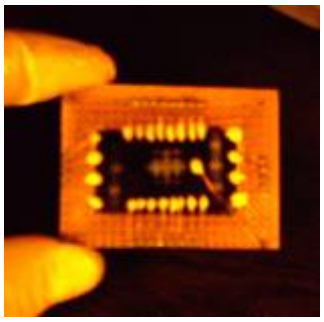

Figure 2.31. PLED sample is attached to FR4 for demo

2.8. Passive Matrix Display Driving Circuit

Generally in flat panel display, column and row electrode arrays are placed perpendicular to each other forming a matrix. When cathode line is connected to ground and anode layer is positively biased, the cell at the intersection of these two electrodes becomes forward biased and emits light. By scanning the rows of the matrix display and applying image data to the columns, any image can be created on the display. For example, in Figure 2.32, second, fifth, sixth, seventh columns and fifth row is triggered. Then on the display one point and a dash is displayed as a frame. By sending different frames

consequent to each other, animated images can be produced. Also, row column synchronization is vital and the scanning rate of must faster that human eye response (above 50 Hz) is needed.

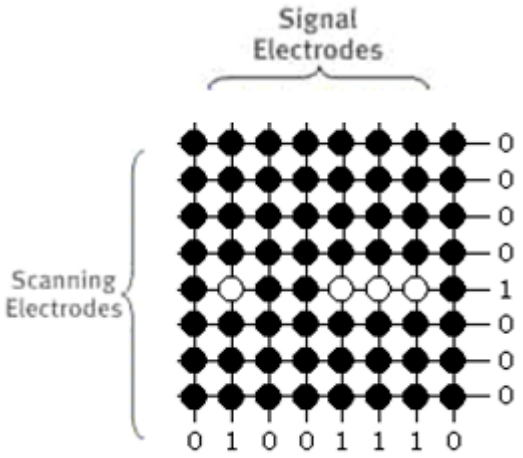

Figure 2.32. Matrix LED display

To drive passive matrix polymer display, programmable integrated circuit (PIC) based driver circuit is designed, Figure 2.33. With this circuit any alphanumeric fonts can be displayed and graphical animations can be demonstrated on eight by eight matrix display. The graphical information can be changed with PC connection via serial port.

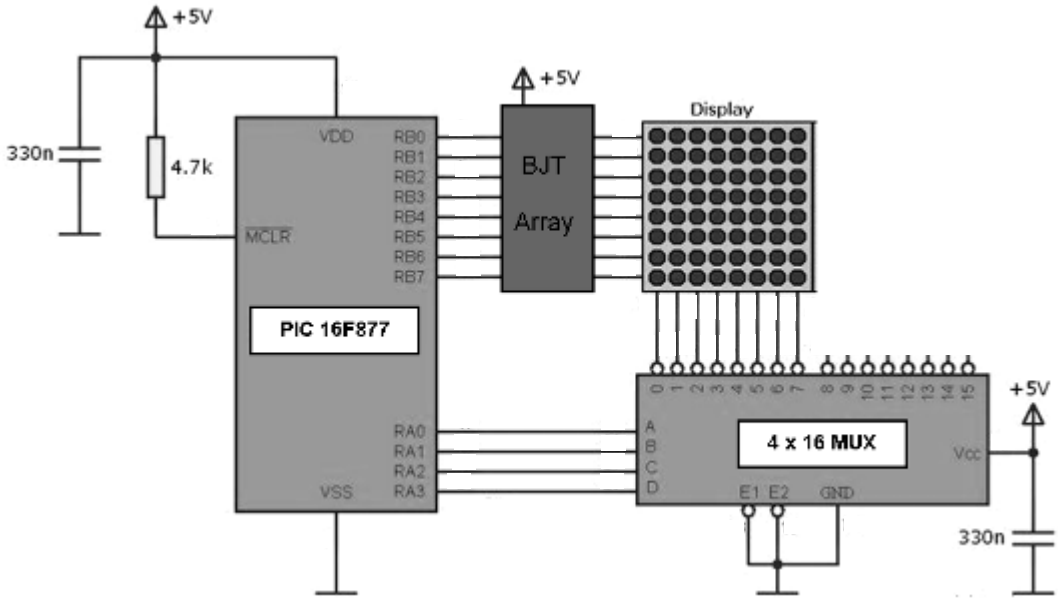

Figure 2.33. Passive matrix polymer display driving circuit

Five by seven solid-state LED matrix displays are used to test the driving circuit and the written assembly program, as shown in Figure 2.34. The related program codes are

given in appendix section. The letter frames are loaded to displays sequentially and each frame appears approximately one second.

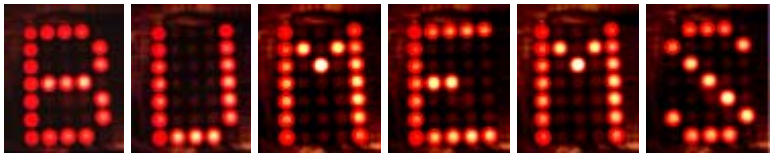

Figure 2.34. Testing of driver circuit with solid state 5x7 matrix display

By driving discrete inorganic LEDs with the driving circuit, any letter or figure could be displayed. Similarly any letter or figure can be displayed using PLEDs by patterning only the anode (ITO) electrode as shown in Figure 2.35 and 2.36, . The uniformity and the brightness of these devices are not good because the pictures are taken before the treatment process. After the treatment, the turn on voltage is decreased and the uniformity is improved.

Figure 2.35. Shinning polymer light emitting diode made by anode patterning

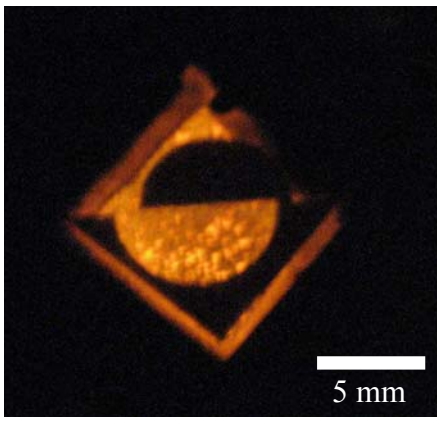

Figure 2.36. Logo of Boğaziçi University is made by polymer light emitting diode

3. TREATMENT & CHARACTERIZATION

3.1. Treatment of Polymer Light Emitting Diodes

Treatment of polymer diodes means regeneration of their electrical and electroluminescent characteristics after they have degraded by special methods. As it is given in previous chapters polymer based devices have excellent properties such as easy manufacturing and modification and low cost, however, when compared to their inorganic counterparts, polymer semiconducting devices currently have lower performances, less reliability and shorter lifetimes [91, 92, 93]. The main reason for this is the fast degradation nature of these polymers under oxygen and water vapor environment.

Therefore, polymer semiconducting devices still need more study on the refinement of their fabrication and characterization, testing of their performances and post fabrication treatments for performance improvement. Several groups have studied performance improvement and stability of organic materials used in polymer light emitting devices [94-97] and solar cells [98, 99]. In these studies, in order to increase the performance of polymer or to prevent contamination of semiconducting devices all fabrication steps are done in an inert environment like nitrogen or argon. Similarly they have applied different treatment methodologies at some point of the fabrication process like UV ozone or chemical treatments applied to ITO or conducting polymers [94-99].

We investigate two different treatment methodologies; heat treatment and electrical treatment. Treatment procedure is applied to samples at the end of the fabrication process. Organic semiconductors are sensitive to the oxygen and humidity. However, in our production, all fabrication steps are realized at ordinary room conditions. Therefore, the device performance might be poor compared to the products that are produced in highly controlled clean room environment. Due to the contamination of polymer layer during the fabrication, the junctions do not behave like a diode or emit light. The treatment process is applied after fabrication and wiring but before encapsulation as shown in Figure 3.1, which is a flow chart giving the fabrication process steps in order. The electrical behavior of diode is revived, and device starts to emit light after heat treatment and its efficiency is improved after electrical field treatment following the heat treatment.

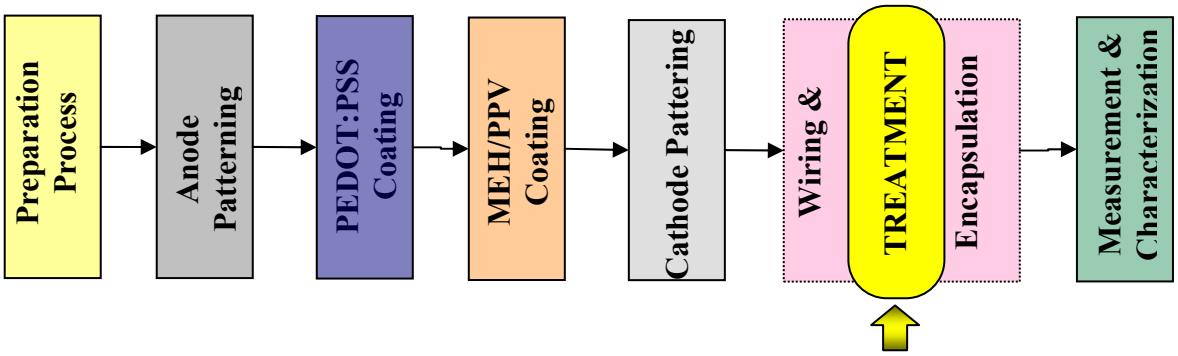

Figure 3.1. Process flow chart showing the order of the treatment step in fabrication flow

Electrical treatment, or voltage treatment, is applied after the heat treatment. The temperature of the device is not changed during voltage treatment stage, as shown in Figure 4.2. Various temperature levels are tested in heat treatment stage. After optimum temperature level is found at the end of the first stage, in the second step, electrical field treatment is done at that specific temperature. Different voltage levels are tested in electrical treatment process. Results obtained from treated devices are given in the following sections.

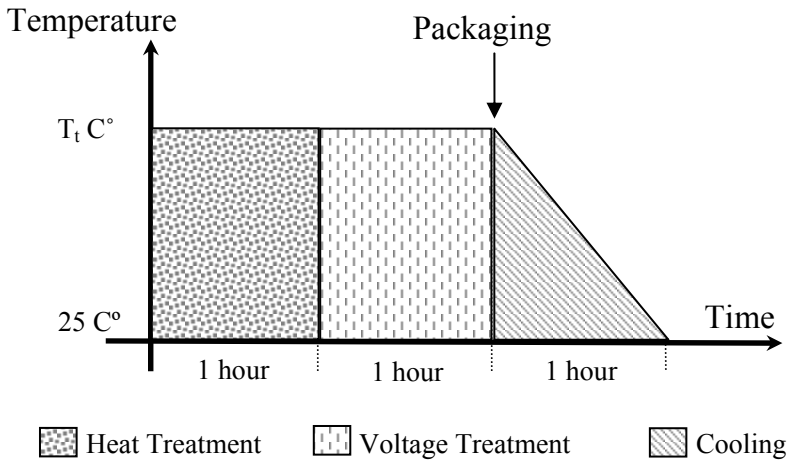

Figure 3.2. Sample temperature during treatment processes

3.1.1. Heat Treatment

Heat treatment is done for a specific duration on a hotplate. The set-up is shown in Figure 3.3, which is at a specific temperature and is in a low vacuum nitrogen environment. Nitrogen-vacuum environment is obtained first by filling the desiccators with nitrogen then vacuuming by a vacuum pump. Two repetitions of fill and purge process are

done. Due to low humidity and oxygen environment and high temperature, most of the absorbed contaminants like oxygen and water vapors inside the devices are removed in this treatment step.

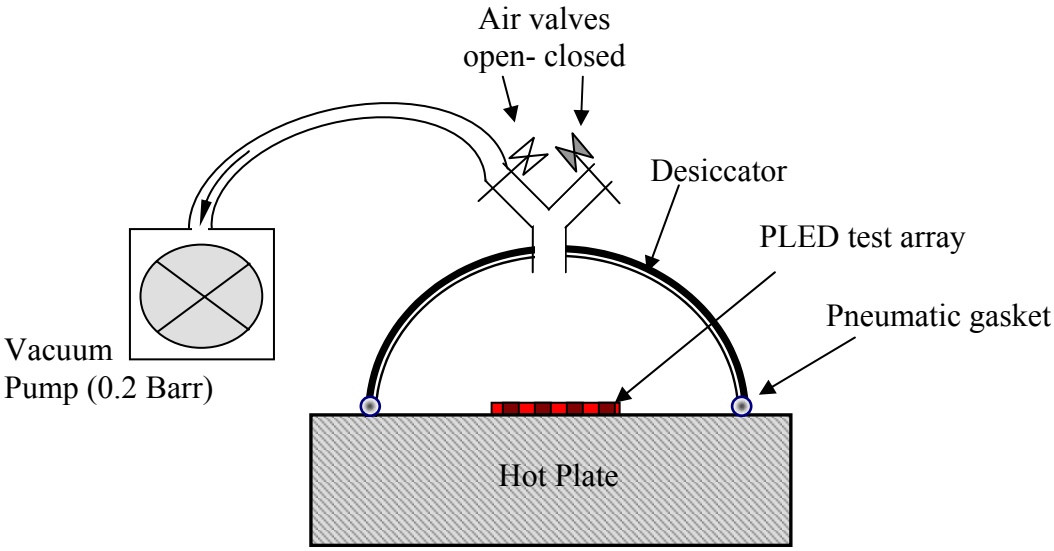

Figure 3.3. Experiment set-up for heat treatment

In heat treatment process to find the optimum temperature, couple 3x3mm^2 square PLED cells are extracted from the wafer with close proximity. This eliminates the effects of process variations from one batch to another. Therefore, the treatment is tested using identical samples. The duration of temperature annealing is proposed as one hour. At the end of the experimental trials, no significant further improvement is observed after one hour as proposed in literature also [95]. Temperature is not increased firmly to minimize the surface tensions between the layers. Treatment is done under 0.2 bar vacuum in dark environment.

Four different temperature levels are tested in heat treatment stage. As it can be observed from the results shown Figure 3.4, the optimum temperature for heat treatment is found as 150 ˚C.

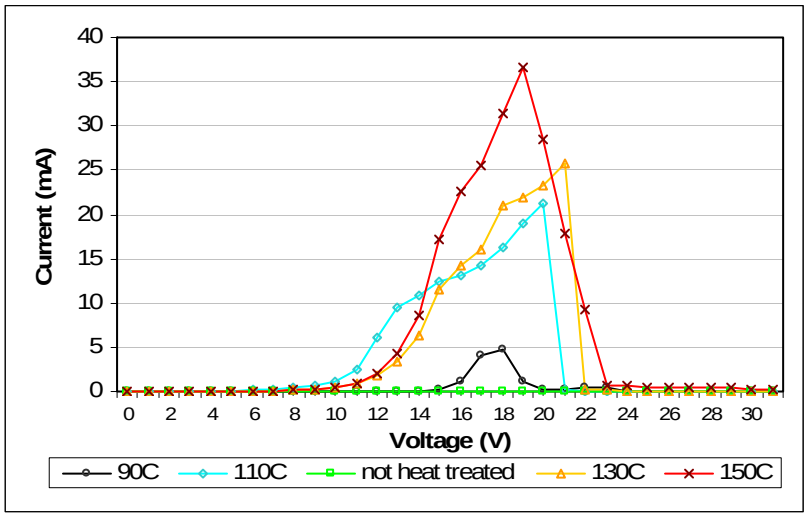

Figure 3.4. Effect of treatment temperature on I-V curve of PLED

The optical characteristic of PLED, treated with different temperature, is determined with an optical set-up composed of equipments purchased from Ocean Optics. For relative measurements, bare fiber optic probe is used. For absolute measurements integrating sphere (IS) is used to capture total luminous emitted from the device. Fiber optic probe with 200 μm radius is used to determine the light spectrum of PLEDs. Usually, relative measurements are made with fiber optic probe because light with low intensities is lost in IS. Measurements made with fiber optic probe are more sensitive. The luminance measurement made with fiber optic probe gives the result in $\mu W/cm^2/nm$ on a personal computer (PC) communicating with Fiber Optic Spectrometer (USB 4000 from Ocean Optics). The spectrometer is configured for the visible range (VIS). Moreover, the calibration of the spectrometer must be accomplished before the measurements. Calibrations must be according to the type of sensing devices used such as bare fiber, fiber plus cosine corrector, or an integrating sphere. For absolute measurements Fiber Optic Integrating Sphere (FOIS-1) is used. One side of the optical fiber is attached to integrating sphere (IS) and the other side is connected to the Fiber optic spectrometer. Calibrations are done with a calibrated light source (LS-1-CAL-INT).

Both the electrical and luminance measurements show that the treatment at 150 C° gives better performance, Figure 3.5. However, due to physical stress on device and operation difficulties for PET substrate above 130 C°, 130 C° is selected as an optimum temperature level for heat treatment.

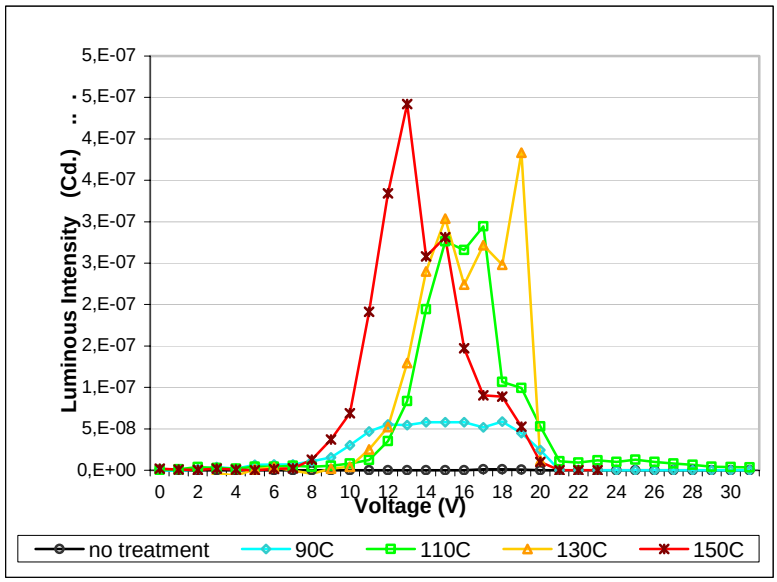

Figure 3.5.Effect of treatment temperature on luminous intensity

If we look at the absolute measurements of the samples with 5 mm x 5 mm dimensions, they consume 108 mW power at 13.5 Volts. On dropping the voltage across the ~100 ohms resistance of ITO, due to sheet resistance, the total electrical power consumed is equal to 100 mW. From the optical measurement luminous intensity is found as 2.41 mCd and illuminance is 30.3 mlx. These values are relatively low because of low coupling efficiency of our device and blocked light by the device itself inside the integrating sphere. For the front encapsulation thick (1 mm) glass wafer is attached to the PET side of PLED. Therefore, due to internal reflections inside the glass, glue, and PET, coupling efficiency decreases dramatically. On the other hand, the calibration of the integrating sphere is done without the physical presence of PLED device. However, during the emission of PLED there is nontransparent substrate inside the sphere. This also reduces the magnitude of optical values measured. Electroluminescent efficiency of PLED is reported as 3 lm/W. Our efficiency is 0.28 lm/W without making corrections. After the corrections the performance of the system becomes comparable with the devices in literature. The output spectrum of the devices is given Figure 3.6. In agreement with the works in literature peak emissions is observed near 600 nm.

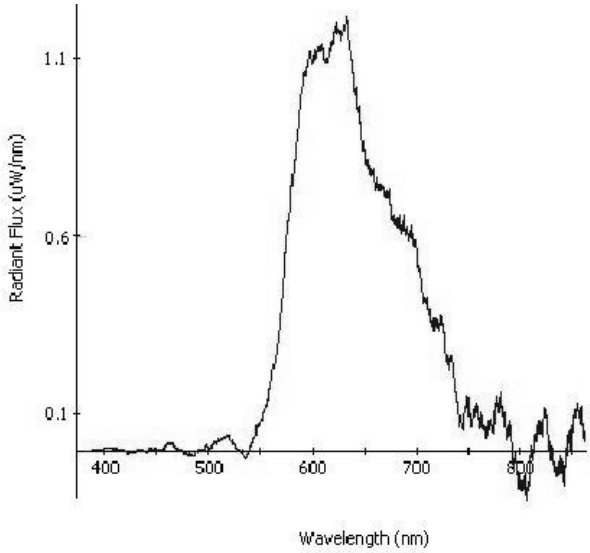

Figure 3.6. Light spectrum of heat treated sample

3.1.2. Electrical Treatment

Electric field treatment is realized consecutive to the heat treatment stage without releasing the vacuum. Since before the heat process started samples are wire bonded, these wires are fed through the desiccators to voltage sources without affecting vacuum, as shown in Figure 3.7.a, b, c. Both negative and positive voltage levels are tested.

3.1.2.1. Forward Bias Electric Treatment When the samples are treated with positive voltages, no electrical improvement is observed on PLED samples. One of the key performance indicators of polymer LEDs is the turn-on voltage and this does not change with electrical treatment, as shown in Figure 3.8. Moreover, if the voltage above the turn voltage is applied to diodes, the samples start shining during treatment. The light remains on for approximately 10 minutes, and then the junction is broken down. After these samples are packaged, no luminance is observed on forward biasing them. Therefore, no improvement is observed after treating polymer light emitting diodes with positive voltages.

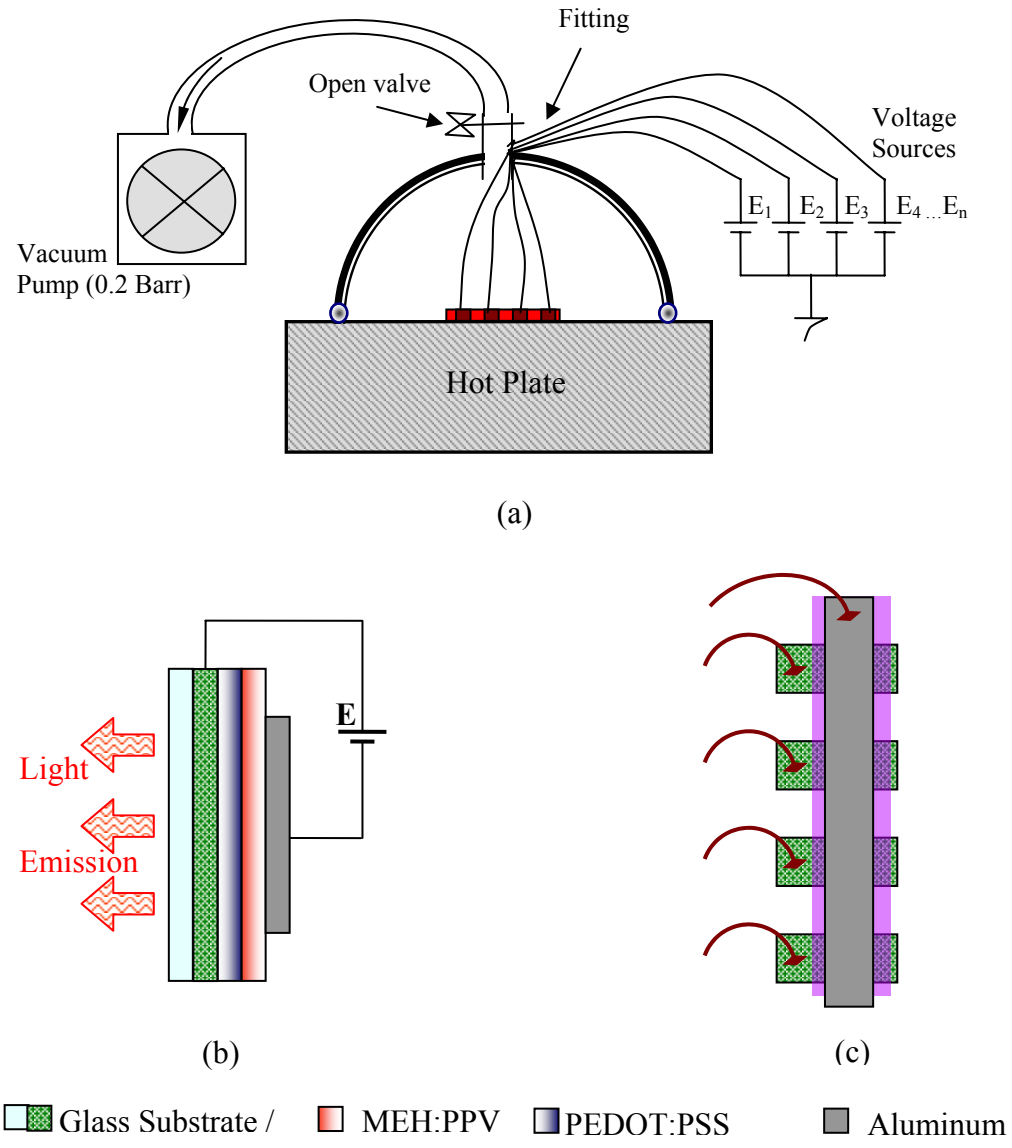

Figure 3.7. a) Experiment set-up for electrical treatment b) Cross sectional view of the junction c) Top view of the wire bonded samples

Similar to the effect of positive voltage treatment on electroluminescent characteristics, samples treated with positive voltage did not show any measurable photovoltaic properties. Independent of the intensity of the applied light, it generates noisy open circuit output voltage and almost zero short circuits current.

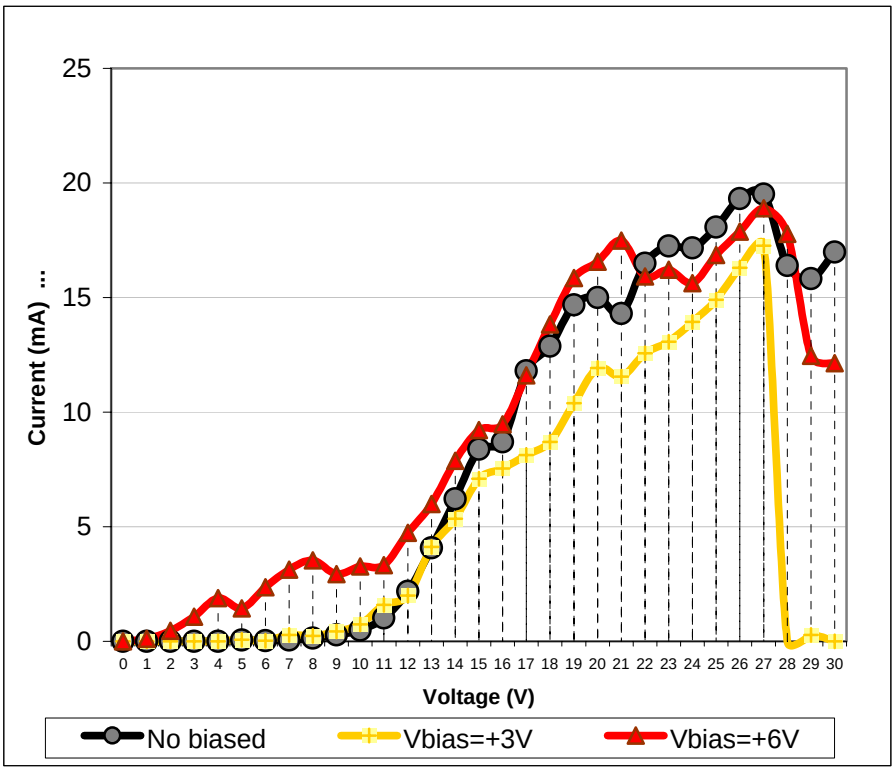

Figure 3.8. Effect of positive voltage treatment on I-V curve of PLED

3.1.2.2. Reverse Bias Electric Treatment Set-up for reverse bias electric treatment is same as the forward one. The only difference is the polarity of the treating voltage sources. There is an obvious improvement observed in both electroluminescence and photovoltaic response of the polymer light emitting diodes upon negative voltage treatment.

3.1.2.2.1.Electroluminescence Response The effects of electric field treatments are tested on both light emitting and photovoltaic properties of PLEDs. Its effect on light emission can be seen in Figure 3.9. For the devices that have been heat treated but not voltage treated as shown as unbiased cell, shown on the column named “No bias” in that figure, the turn voltage is relatively high and the uniformity is very poor. By applying negative electric field to the junctions after the fabrication and heat treatment, the turn-on voltage of the PLED drops down to lower levels. These turn-on voltages increase slowly with the magnitude of the negative treatment voltage. For example, for a device that experienced only heat treatment (No bias column in Figure 3.9) has a turn-on voltage of around 11 volts. However, a device that experienced both heat treatment and an electric field treatment with -1 volts (-1 column in Figure 3.9), has a turn-on voltage of around 4 volts. A device that is treated with -5 volts (-5 column in Figure 3.9), has a turn-on voltage of

around 5 volts. This is also true for the voltage levels where PLEDs shine maximum. In both of the fabrication and treatment trials, independent of the thickness of the polymer films, turn-on and maximum illumination voltage levels are stabilized depending on the bias voltage values of the electric field treatment. For the unbiased cells these voltage levels vary. They are unstable and can not be controlled. Another advantage of electric field treatment is that the uniformity of the light emitting surface is improved.

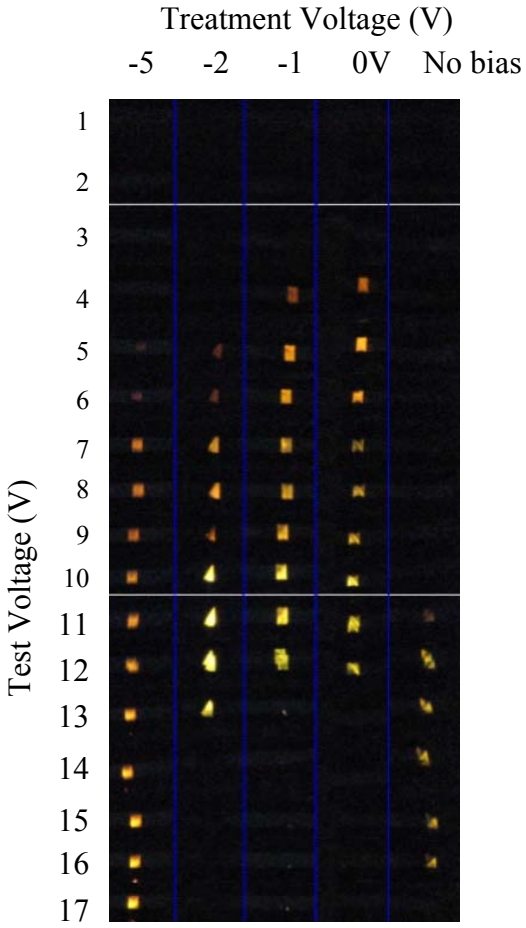

Figure 3.9. Electric field treated rows of PLED samples

Another point about the voltage treatment process is that if the voltage bias applied during treatment stage is not stopped before the cooling, the performance of the polymer light emitting devices significantly degrades. Therefore, the wire connection between voltage supply and polymer junctions must be removed before the cooling stage starts. Although the reason is still under investigation, we believe that the molecular arrangement of the polymeric chains may be disturbed by the applied electric field when the

temperature is under the Tg (65ºC) of MEH-PPV (Mn =400 000, Mw = 626 000) [100] but is above the Tg (40ºC) of PEDOT:PSS [101].

3.1.2.2.2.Photovoltaic Response Photovoltaic response of the PLEDs is tested by measuring open circuit voltage and short circuit current in both dark environment and under the light source of a solar simulator with an intensity of 500 W/m2. Figure 3.10 shows the open circuit voltage response of the heat treated but not electrically treated PET/ITO/MEH-PPV/PEDOT:PSS/Al PLED. The measured voltage is noisy and its average value when exposed to light is very small. On the other hand, after electric field treatment is applied the output voltage of the polymer device as shown in the same figure, is stabilized at a certain level and its average value (55 mV for -1 volt treatment) is an order of magnitude higher than the untreated (heat treated but not electric field treated) ones (5 mV). Similar to the open circuit voltage characteristics of the treated and untreated samples, short circuit current performances are enhanced significantly after the electric field treatment. The results are shown in Figure 3.11. Before the electric field treatment, the short circuit response of the device when exposed to light can not be distinguished from the dark response. However, after the electric field treatment, the intensity of the light shined on the device can be easily detected from its short circuit response (6 nA for -1 volt treatment).

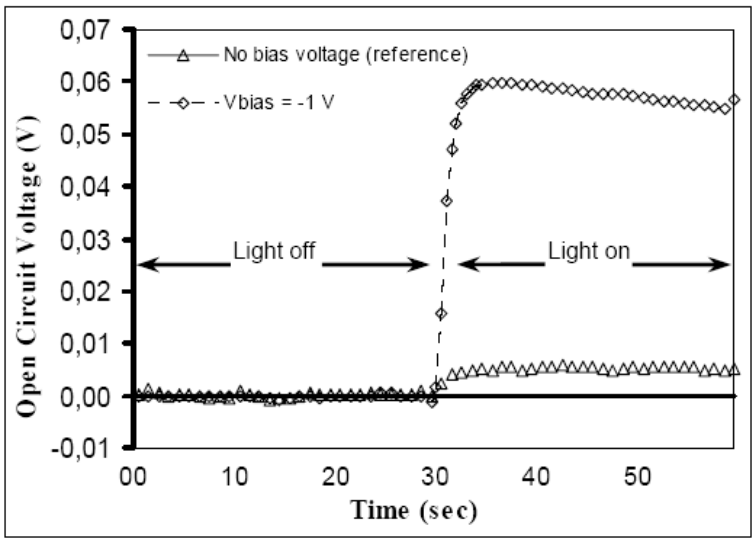

Figure 3.10.Effect of electric field treatment to the open circuit voltage

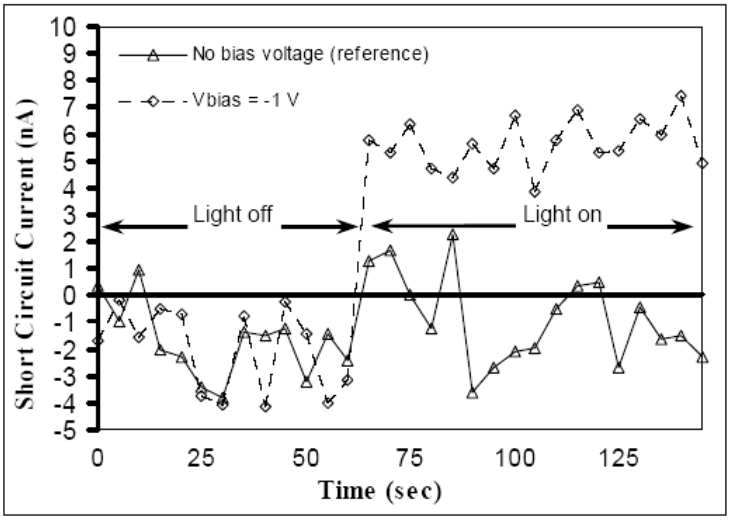

Figure 3.11.Effect of electric field treatment to the short circuit current

The average open circuit voltage and average short circuit current obtained from electric field treated samples are strongly depended on the treatment voltages, Figure 3.12.a and 3.12.b. The averages and standard deviations of the photovoltaic responses of junction are shown in these figures.

The operation of the devices, which were treated at negative voltages, is more stable because they have a mean distant greater than the variance. For example, in Figure 3.12.a samples treated with -1V or -2V are very stable, and their electrical responses are easily measurable when they are used as photodetector. It is worth mentioning that these improvements in the photovoltaic operations of PLEDs due to the electric field treatment also improve their light emitting operation as shown in the previous section. These results are significant since they show that when right electric field treatment is applied to PLEDs after fabrication, they can also be used as photodetector at the same time.

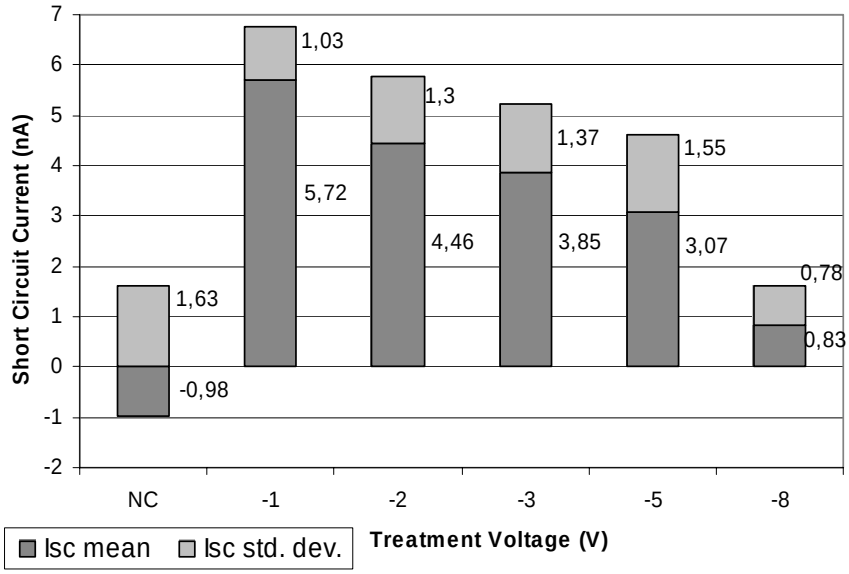

(a)

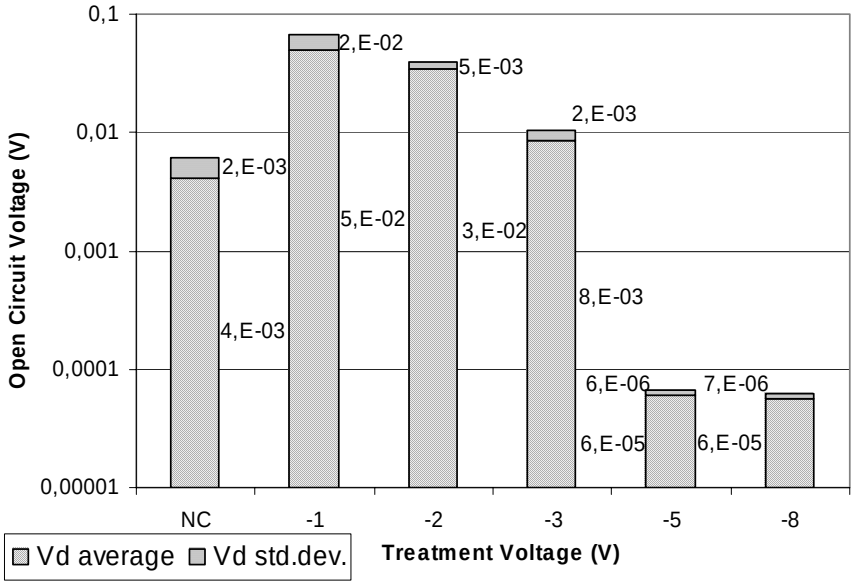

(b)

Figure 3.12. The effect of treatment voltages on the photovoltaic response of PLED a) Short circuit current, b) Open circuit voltages

3.2. Encapsulation

Since in this work we have tested the effectiveness of the developed treatment methodology, flexibility and physical dimensions are not considered important. Therefore, for the front side encapsulation one millimeter thick glass plate is attached with water clear

epoxy or instant drying glue to the PET side of the polymer light emitting diode. Front side encapsulation is made just after the fabrication and before the treatment process.

For the back side encapsulation, bulky hot melt silicone from Henkel is applied to aluminum deposited side of the sample. The encapsulation is realized under vacuum that is sustained during the treatment process. For good backside encapsulation, the temperature of the sample must be as high as possible for the reduction of the bubbles occurred during dispensing of silicon. After the encapsulation the system is cooled to room temperature.

3.3. Lifetime

Although the lifetime of the polymer based system is not compatible to inorganic systems, they must have sufficient lifetime to be able used in commercial products. By making periodic photometric measurements, performance versus time graph is obtained, Figure 3.13. The lifetime of the PLED is found as 400 hours, where the output intensity drops to half of the initial value.

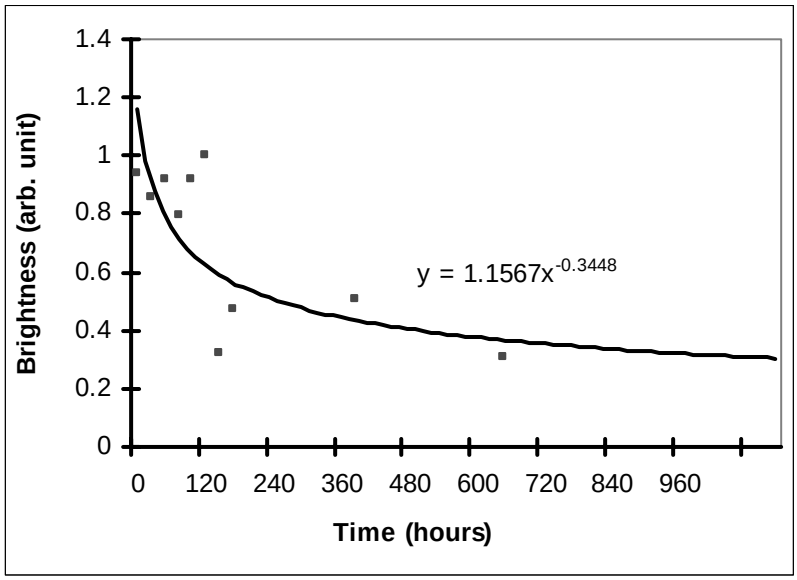

Figure 3.13. Results of lifetime measurements

4. CONCLUSION & FUTURE WORKS

4.1. Conclusion

In this work, the procedure of the fabrication and testing of polymer light emitting diode is given. Each step is characterized and external factors that influence the process are determined carefully. After the fabrication process, a novel treatment methodology is applied to polymer cells in addition to traditional heat treatment process. The effects of heat treatment and an electric field treatment applied after that on PLEDs have been investigated. These treatments are done at the end of the fabrication after wiring, which makes fabrication easier and more feasible. After the fabrication of square test cells heat treatment is performed at 130C^{o}, which is greater than glass transition temperature, Tg, of MEH-PPV for one hour. Electric field treatment is realized afterwards with positive and negative voltage levels. In the fabrication of PLEDs, no preventive measures are taken against exposure to oxygen and water vapors, which make the fabrication significantly cheaper. Heat treatment after fabrication followed by packaging in the same conditions restores the light emitting properties of otherwise not functioning PLEDs. It removes the absorbed oxygen and water vapors inside the devices rendering them functional again. Devices that did not receive any post fabrication treatment did not show any light emitting or photovoltaic properties.

Electric field treatment after heat treatment is applied to PLEDs in reverse bias for the first time in this work. Light emitting and photovoltaic properties of PLEDs are improved compared to devices that are treated with heat only. Electric field treatment after heat treatment lowers the turn on voltage levels and the levels at which PLED reaches its maximum luminescence when used as a light emitting device. Turn-on voltage of a PLED

drops to 4 volts when treated with -1 volt in comparison to 11 volts when treated with heat only. When PLED is used as a photovoltaic device, its average value of the short circuit current and open circuit voltage increases by one order of magnitude compared to the values of the devices treated with heat only. Under 500mW/m^2 light intensity, 5 mV open circuit voltage and 0.5 nA short circuit current values with heat treatment only improve to 55 mV and 5 nA respectively after electrically treated with -1 volt. Furthermore, the uniformity of the light emitting surface increases significantly after electric field treatment.

Initially applied heat treatment removes most of oxygen and water vapors PLEDs absorbed during fabrication steps, which degrade the junction and quenching the photons. Moreover, by heating the polymer pinholes on polymer layer is filled and local short circuits are reduced. This explains how the light emitting property of a PLED can be restored with a heat treatment only step. Further improvement of both the light emitting and photovoltaic functions of PLED by the electric field treatment after heat treatment can be explained by the alignment of the polymer chains. It is proposed that above the glass transition temperatures since the polymer chains become mobile, they are reoriented by the applied electric field resulting in a more uniform structure. This new arrangement improves the chemical bonding between interfacial junctions lowering or eliminating potential barriers due to contaminants or other non idealities. It may also create zones of space charges close to PEDOT:PSS. These created space charges lower the number of injected holes. This is advantageous because it creates a balance between the number of injected holes and electrons. The number of injected electrons are already low especially due to the high energy barrier between the LUMO of MEH-PPV and work function of aluminum. However, the new arrangement after electric field treatment increases the efficiency of the PLED by decreasing the number of injected hole carriers, thus improving the balance between electrons and holes injected towards the electroluminescent polymer.

Although the heat treatment by itself is not enough to make PLEDs function as a photodetector, the electric treatment following the heat treatment makes devices usable as photodetectors as well as light emitting devices. In both of the fabrication and treatment trials, independent of the thickness of the polymer films, turn-on and maximum illumination voltage levels are stabilized depending on the bias voltage values applied during the electric field treatment.

4.2. Future Work

To obtain higher performance from PLEDs, the fabrication must be realized in inert environment provided by glove box system. If the devices are never exposed to the air, the efficiency of the devices will absolutely increase. Moreover, different spectroscopic or thin film related measurements of the PLEDs will be useful to deeply understand the physical and electrical properties of the devices and influences of the external affects. By this way, more realistic model can be derived by considering other parameters like roughness, thickness, reflectance, and other parameters.

On the other hand, experiencing and clarifying advanced polymer micro fabrication methodologies might be useful for the generation of cost effective devices and feasible industrial products. For example, examination of ink-jet printing, soft printing, roll to roll (or off-set printing) manufacturing will be useful for generation of profitable consumer goods.

REFERENCES

1. Scott, J.C. and J.H. Kaufman, P. J. Brock, R. Dipietro, J. Salem, J. A. Goitia, J., Degradation and failure of MEH-PPV light-emitting diodes", Appl. Phys. vol. 79, pp. 2745, 1996

2. Parker, I. D. and Y. Cao, C. Y. Yang, "Lifetime and degradation effects in polymer light-emitting diodes", J. Appl. Phys., vol. 85, pp. 2541, 1999

3. John, J. C., "The future of clean room design", The European Journal of Contamination Control, 2002

4. http://www.microchem.com/products/pdf/SU8_2035-2100.pdf

5. Duffy, D. C., and J. C. McDonald, J. O. J. A. Schueller, G. Whitesides, "Rapid prototyping of microfluidicsystems in poly(dimethylsiloxane)," Analytical Chemistry, v ol. 70, no. 23, , pp. 4974-4984, Dec 1, 1998

6. Man, P. F. and D. K. Jones, C. H. Mastrangelo, "Microfluidic plastic capillaries on silicon substrates: a new inexpensive technology for bioanalysis chips," Proceedings of the IEEE. Micro Electro Mechanical Systems (MEMS), pp. 311-316, 1997

7. Senol, M. and F. Svec, C. H. Mastrangelo, J. M. J. Frechet, Y. B. Gianchandani, "Enhanced Electro-Osmotic Pumping With Liquid Bridge and Field Effect Flow Rectification," Presented in IEEE MEMS 2004 Conference, Maastricht, The Netherlands, pp. 850-853, 2004

8. Hilt, J. Z. and J. Z. A. K. Gupta, R. Bashir, N. A. Peppas, "Ultrasensitive BioMEMS sensors based on microcantilevers patterned with environmentally responsive hydrogels," Biomedical Microdevices, vol. 5, is. 3, pp. 177-84, 2003

9. Luo, Q. and S. Mutlu, Y. B. Gianchandani, F. Svec, J. M. J. Frechet, "Monolithic Valves For Microfluidic Chips Based On Thermoresponsive Polymer Gels", Electrophoresis, vol. 24, pp. 3694-3702, 2003

10. Brittain, S. and K. Paul, Z. Xiao-Mei, G. Whitesides, “Soft lithography and microfabrication”, Physics World, vol. 11, no. 5, , pp. 31-36, May 1998.

11. Yang, G. and G. Srdanov, W. Hailiang, C. Yong, A. J. Heeger, “High-performance polymer photovoltaic cells and photodetectors”, Proceedings of the SPIE - The International Society for Optical Engineering, vol. 4108, pp. 48-56, 2001

12. Dobbertin, T. and E. Becker, T. Benstem, G. Ginev, D. Heithecker, H.-H. Johannes, D. Metzdorf, H. Neuner, R. Parashkov, W. Kowalsky, “OLED matrix displays: in-line process technology and fundamentals” T. Dobbertin et al., Thin Solid Films pp.132–139, 2003

13. Rogers, J. A. and Z. Bao, K. Baldwin, A. Dodabalapur, B. Crone, V. R. Raju, V. Kuck, H. Katz, K. Amundson, J. Ewing, P. Drzaic, “Paper-like electronic displays: Large-area rubber-stamped plastic sheets of electronics and microcapsulated electrophoretic inks”, Proceedings of the National Academy of Sciences of the United States of America (PNAS), vol.98, no. 9, pp. 4835-4840, 2001

14. Vulto, S. I. E. and M. Buchel, P. C.Duineveld, F. Dijksman, M. Hack, M. Kilitziraki, M. M. de Kok, E. A. Meulenkamp, J.-E. Rubingh, P. van de Weijer, S. H. P. M. de Winter, “Technology and materials for full-color polymer light-emitting displays”, Proceedings of the SPIE - The International Society for Optical Engineering, vol. 5214, no. 1, pp. 40-49, 2004

15. Gustafuson, G. and Y. Cao, G.M. Treacy, F. Klavetter, N. Colaneri, A. J. Heeger, Nature, vol. 357, pp. 477, 1992

16. NanoMarkets, LC, A company providing research services and reports for the analysis of thin film, organic and printable electronics related industry, market and technology, 2007

17. Janice, K. M. “History and Status of Organic Light Emitting Device (OLED) Technology for Vehicular Applications”, SID Symposium Digest of Technical Papers, vol. 32, is. 1, pp. 22-25, 2001

18. Padinger, F. and C. J. Brabec, T. Fromherz1, J. C. Hummelen, N. S. Sariciftci, “Fabrication of large area photovoltaic devices containing various blends of polymer

and fullerene derivatives by using the doctor blade technique", Opto-Electronics Review 8 vol. 4, pp.280-283, 2000

19. Hack, M. and A. Chwang, Y.-J. Tung, R. Hewitt, J. Brown, J.-P. Lu, C. Shin, J. Ho, R. A. Street, L. Moro, X. Chu, T. Krajewski, N. Rutherford, R. Visser, "Status and Opportunities for High Efficiency OLED Displays on Flexible Substrates", Materials Research Society, Preceding Papers, 2005

20. Horning, R. and B. Johnson, "Polymer-based MEMS actuators for biomimetics." The Proceedings of Neurotechnology for Biomimetic Robots, MIT Press, 2002

21. Chan, L., "Recent developments in polymer MEMS", Advanced Materials, vol. 19, no. 22, pp. 3783-3790, 2007

22. Huang, J. and X. Wang, A. J. deMello, J. C. deMello, D. D. C. Bradley, "Efficient flexible polymer light emitting diodes with conducting polymer anodes", J. Mater. Chem., vol. 17, pp. 3551-3554, 2007

23. Yang, S. and G. C. Bazan, A. J. Heeger, "Long-lifetime polymer light-emitting electrochemical cells", Adv. Mater., vol. 19, pp. 365–370, 2007

24. Zou, D. and M. Yahiro, and T. Tsutsui, "Voltage shift phenomena introduced by reverse-bias applicationin multilayer organic light emitting diodes", Appl. Phys. Lett. vol. 72, pp. 2484, 2000

25. Atreyaa, M. and S. Lia, E. T. Kanga, K. G. Neoha, Z. H. Mab, K. L. Tanb, W. Huangc, "Stability studies of poly (2-methoxy-5- (2′-ethyl hexyloxy) -p- (phenylene vinylene) [MEH-PPV]" Polymer Degradation and Stability, vol. 65, is. 2, pp.287-296, 1999

26. Petr, A. and F. Zhang, H. Peisert, M. Knupfer, L. Dunsch, "Electrochemical adjustment of the work function of a conducting polymer", Chemical Physics Letters vol. 385, pp. 140–143, January 2004

27. Zhong, Z. Y. and Y. D. Jiang, "Surface modification and characterization of indium–tin oxide for organic light-emitting devices", Journal of Colloid and Interface Science, vol. 302, pp. 613–619, August 2006

28. Tengstedt, C. and A. Kanciurzewska, M. P. de Jong, S. Braun, W. R. Salaneck, M. Fahlman, “Ultraviolet light–ozone treatment of poly(3,4-ethylenedioxy-thiophene)-based materials resulting in increased work functions”, Thin Solid Films, vol. 515, is. 4, pp.2085–2090, August 2006

29. Songa, M. Y. and D. K. Kimb, S. M. Jo, D. Y. Kim, “Enhancement of the photocurrent generation in dye-sensitized solar cell based on electrospun TiO2 electrode by surface treatment”, Synthetic Metals , vol. 155, pp. 635–638, 2005

30. Jin, H. and Y. Hou, X. Meng, Y. Li, Q. Shi, F. Teng, “Enhanced photovoltaic properties of polymer–fullerene bulk heterojunction solar cells by thermal annealing”, Solid State Communications, vol. 142, pp. 181–184, 2007

31. Padinger, F. and R. S. Rittberger, N. S. Sariciftci, “Effects of postfabrication treatment on plastic solar cells”, Adv. Func. Matter, vol. 13, no.1, 2003

32. Ma1 D. and J. M. Lupton, R. Beavington, P.L. Burn, I. D. W. Samuel1, “Improvement of luminescence efficiency by electrical annealing in single-layer organic light-emitting diodes based on a conjugated dendrimer”, J. Phys. D: Appl. Phys. vol. 35, pp.520-523, 2002

33. Yahiro, M. and D. Zou, T. Tsutsui, “Recoverable degradation phenomena of quantum efficiency in organic EL devices”, Synthetic Metals, vol. 112, pp. 245-247, 2000

34. Bernanose, A. and M. Comte, P. Vouaux, “A new method of emission of light by certain organic compunds”, J. Chem. Phys., vol. 50, pp. 64-68, 1953

35. Bernanose, A., “The mechanism of organic electroluminescence”, J. Chem. Phys., vol. 52, pp. 396-400, 1955

36. Hartman, W. A. and H. L. Armstrong, “Photoluminescence in polymeric insulating materials (low densitypolyethylene and polypropylene) induced by ultraviolet photons”, J. Appl. Phys., vol. 38, pp. 2393, 1967

37. Round, H. J., “A note on carborundum”, Electron. World, vol. 19, pp. 309-310, 1907

38. Holonyak, N. Jr. and S. F. Bevacqua, “Coherent (visible) light emission from $Ga(As_{1x}P_x)$ junctions”, Appl. Phys. Lett., vol. 1, pp.82-83, 1962

39. Perry, T. S., “Red hot”, IEEE Spectrum, June 3, 2003

40. Pope M.,and H. Kallman, P. Magnante, “Electroluminescence in organic crystals”, J. Chem. Phys., vol. 38, 2042-2043, 1963

41. www.pioneerelectronics.com, Press Releases, 1999

42. www.kodak.com, Press Releases, 2003

43. Chiang, C. K. and C. R. Fincher, Y. W. Park, A. J. Heeger, H. Shirakawa, E. J. Louis, S. C. Gau, A. G. Macdiarmid, “Electrical conductivity in doped polyacetylene”, Phys. Rev. Lett., vol. 39, pp. 1098-1101, 1977

44. Heeger, S. and E. J. Louis, A. G. Macdiarmid, C. K. Chiang, A. J. Heeger, “Synthesis of electrically conducting organic polymers: halogen derivatives of polyacetylene, $(CH)_x$”, Chem. Commun., vol. 16, pp. 578-580, 1977

45. McGehee, M. D. and E. K. Miller, D. Moses, A. J. Heeger, “Twenty years of conducting polymers: from fundamental science to applications in Advanced Synthetic Metals: Twenty years of progress in science and technology”, P. Bernier, S. Lefrant, G. Bidan, Eds. Elsevier, Amsterdam, pp. 98-205, 1999

46. Kiebooms, R. and R. Menon, K. Lee, “Synthesis, electrical and optical properties of conjugated polymers”, Handbook of advanced electronic and photonic materials and devices, H. S. Nalwa, Ed., Academic Press, New York, pp. 1-102, 2001

47. Tomozawa, H. and D. Braun, S. D. Philips, A. J. Heeger, H. Kroemer, “Metal-polymer shoottky barriers on cast films of soluble poly(3-alkylthiophenes), Synth. Met., vol. 22, pp.63-69, 1987

48. John, H. B. and D. D. C. Bradley, A. R. Brown, R. N. Marks, K. Mackay, R. H. Friend, P. L. Burns, A. b. Holmes, “Light-emitting diodes based on conjugated polymers”, Nature, vol. 347, pp. 539-541, 1990

49. Donald, B. and A. J. Heeger, “Visible light emission from semiconducting polymer diodes”, Appl. Phys. Lett., vol. 58, pp. 1984-1991

50. Wudl, F. and P-L. Allemand, G. Srdanov, Z. Ni, D. McBranch, “Polymer and an unusual molecular crystal with NLO properties”, Materials for Nonlinear optics:

Chemical Perspectives, S. R. Marder, J. E. Sohn, G. D. Stucky, Eds., American Chemical Society, pp. 683-686, 1991

51. Becker, H. and H. Spreitzer, K. Ibrom, W. Kreuder, "New insights into microstructure of lich polymerized PPVs", Macromolecules, vol. 32, pp. 4925-4932, 1999

52. Gang, Y. and A. J. Heeger, "Semiconducting polymers as materials for device applications", The physics of semiconductors, M. Schleffer, R. Zimmerman, Eds. World Scientific, pp. 355, 1996

53. Chang, Z. and G. Yu, Y. Cao, "Long operating life for polymer light emitting diodes", U.S. Patent 5,798,10, 1998

54. Becker, H. and H. Spreitzer, W. Kreuder, E. Kluge, H. Schenk, I. D. Parker, Y. Cao, "Soluble PPVs with enhanced performance-a mechanistic approach", Adv. Matter, vol. 12, pp. 42-48, 2000

55. Weiss, O. J. and R. Krause, R. Paetzold, "Organic Thin Film Devices for Displays and Lighting", Advances in Solid State Physics, vol. 46, pp. 321-332, 2007

56. Polymer Vision Ltd., Press releases, 22nd January, 2008

57. Pope, M. and C. E. Swenberg, "Electronic processes in crystals and Polymers", Second Edition, Oxford Unniversity Press, NY, 1999

58. Heeger A. J. and S. Kivelson, J. R. Schrieffer, W.-P. Su, Rev. Mod. Phys. vol. 60, pp. 781, 1988

59. Soos, Z. G. and S. Ramasesha, D. S. Galvao, R. G. Kepler, S. Etanad, Syn. Met., vol. 54, pp. 35, 1993

60. Craig, D. P. and S. H. Walmsley, "Excitons in Molecular Crystals", W. A. Benjamin Inc., New York, 1968

61. Pope, M. and C. E. Swenberg, "Electronic processes in organic crystals", Clarendon Press, Oxford Univ. Press, New York, 1982

62. Brown, A. R. and K. Pichler, N. C. Greenham, D. D. C. Bradley, R. H. Friend, A. B. Holmes, “Optical Spectroscopy of triplet excitons and charged excitations in poly(p-phenylenevinylene) light emitting diodes”, Chem. Phys. Lett., vol. 210, pp. 61-66, 1993

63. Baldo, M. A. and C. Adachi, S. R. Forrest, Phys. Rev. vol. 62, pp. 10967, 2000

64. Wilson, J. S. and A. S. Dhoot, A. Seeley, M. S. Khan, A. Kohler, R. H. Friend, Nature, vol. 413, pp. 828, 2001

65. Yang, Y., “Polymer electroluminescent devices”, MRS Bulletin, vol. 22, pp. 31-28

66. Andersson, A. and N. Johansson, P. Bröms, N. Yu, D. Lupo, andW. R. Salaneck, “Fluorine tin oxide as an alternative to indium tin oxide in polymer LEDs”, Adv. Mat., vol. 10, pp. 859–863, 1998

67. Zhu, F. and K. Zhang, C. H. Huan, A. T. Wee, “Effect of ITO carrier concentration in the performance of organic light-emitting diodes,” in Mat. Res. Soc. Symp. Proc., vol. 598, pp. BB11.11.1, 2000

68. Yang, Y. and W. Westerweele, C. Zhang, P. Smith, A. J. Heeger, J. Appl. Phys. vol. 77, pp. 694, 1995

69. Campbell, A. J. and D. D. C. Bradley, and H. Antoniadis, “Quantifying the efficiency of electrodes for positive carrier injection into poly(9,9- dioctylfluorene) and representative copolymers”, J. Appl. Phys, vol. 89, pp. 3343–3351, 2001

70. Savvateev, V. N. and A. V. Yakimov, D. Davidov, R. M. Pogreb, R. Neuman, Y. Avny, Appl. Phys. Lett. vol. 71, pp. 3344, 1997

71. Wang, W. and S. F. Lim, S. J. Chua, JAP, vol. 91, pp. 5712, 2002

72. Deng, X. Y. and M. K. Ho, and K. Y. Wong, “Top-emitting polymer light-emitting diodes with environmentally stable cathodes”, J. Appl. Phys. vol. 99, is. 1, pp. 016103, 2006

73. Andersson, A. and N. Johansson, P. Bröms, N. Yu, D. Lupo, and W. R. Salaneck, “Fluorine tin oxide as an alternative to indium tin oxide in polymer LEDs,” Adv. Mat., vol. 10, pp. 859–863, 1998

74. Fang, Z. and K. Zhang, C. H. Huan, and A. T. Wee, “Effect of ITO carrier concentration in the performance of organic light-emitting diodes,” in Mat. Res. Soc. Symp. Proc., vol. 598, pp. BB11.11.1, 2000

75. Kao, P.C., and S.-Y. Chu, Member, IEEE, T.-Y. Chen, C.-Y. Zhan, F.-C. Hong, C.-Y. Chang, L.-C. Hsu, W.-C. Liao, M.-H. Hon, “Fabrication of Large-Scaled Organic Light Emitting Devices on the Flexible Substrates Using Low-Pressure Imprinting Lithography”, IEEE Transactions On Electron Devices, pp. 0018-9383, 2005

76. http://www.microchemicals.eu/technical-information/photoresist_coating.pdf

77. http://www.microresist.de/products/room_haas/pdf/Microposit_S1800_G2_Serie.pdf

78. Chang, S.C. and S. C. Hsieh, K. U. Shan, T. C. Cheng , B. T. Dai, “Processing and characterization of a positive thick photoresist”, Solid State Technology, Taiwan

79. http://www.photo-sciences.com/

80. http://www.cise.columbia.edu/clean/process/Photolithography_Lessons.pdf

81. Optics, Fourth Edition. Pearson Higher Education, March 2003

82. http://www.matter.org.uk/schools/Content/Refraction/absolute.html

83. Wohlmutha, W. and I. Adesida, “Properties of R.F. magnetron sputtered cadmium–tin–oxide and indium–tin–oxide thin films”, Thin Solid Films, vol. 479, is. 1-2, pp. 223-231, 2005

84. Bashar, S. A., "Study of Indium Tin Oxide (ITO) for Novel Optoelectronic Devices", Ph.D. thesis, ch.. 3, 1998

85. Reddy, V. S. and K. Das, S. K. Ray, A. Dhar, “Characteristics of MEH-PPV thin films on ITO electrode for organic light emitting diodes”, Proc. of ASID, October 2006

86. https://www.memsnet.org/mems/processes/etch.html

87. Chatterjee, S. and M. Ujihara, D. G. Lee, J. Chen, S. Lei, G. P. Carman, "Spray etching 2 μm features in 304 stainless steel", Journal of Micromechanics and Microengineering, vol. 16, no. 12, is.8, pp. 2585-2592, December 2006

88. http://snf.stanford.edu/Process/Lithography/liftoff.html

89. Moran, J. M. and D. Maydan, "High Resolution, Steep Profile Resist Patterns", J. Vac. Sci. Technol., vol. 6, is.60, p.1620,1979

90. Hamel, C. J. and D. R. Weed, "Modified soaking solvent for single resist lift-off structures", IBM-Technical-Disclosure-Bulletin, vol.21, no.8, pp. 3103, January 1979

91. Huang J. and X. Wang, A. J. deMello, J. C. deMello, D. D. C. Bradley, "Efficient flexible polymer light emitting diodes with conducting polymer anodes", J. Mater. Chem., vol. 17, pp. 3551-3554, 2007

92. Shao, Y. and G. C. Bazan, A. J. Heeger, "Long-lifetime polymer light-emitting electrochemical cells", Adv. Mater., vol. 19, pp. 365–370, 2007

93. Zou, D. and M. Yahiro, and T. Tsutsui, "Voltage shift phenomena introduced by reverse-bias applicationin multilayer organic light emitting diodes", Appl. Phys. Lett. 72, 2484 (2000).

94. Atreyaa, M. and S. Lia, E. T. Kanga, K. G. Neoha, Z. H. Mab, K. L. Tanb, W. Huangc, "Stability studies of poly(2-methoxy-5-(2′-ethyl hexyloxy)-p- (phenylene vinylene) [MEH-PPV]" Polymer Degradation and Stability, vol. 65, is. 2, pp.287-296, 1999

95. Peter, A. and F. Zhang, H. Peisert, M. Knupfer, L. Dunsch, "Electrochemical adjustment of the work function of a conducting polymer", Chemical Physics Letters vol. 385, pp. 140–143, January 2004

96. Zhong, Z. Y. and Y. D. Jiang, "Surface modification and characterization of indium–tin oxide for organic light-emitting devices", Journal of Colloid and Interface Science, vol. 302, pp. 613–619, August 2006

97. Tengstedt C. and A. Kanciurzewska, M. P. de Jong, S. Braun, W. R. Salaneck, M. Fahlman, “Ultraviolet light–ozone treatment of poly(3,4-ethylenedioxy-thiophene)-based materials resulting in increased work functions”, Thin Solid Films, vol. 515, is. 4, pp.2085–2090, August 2006

98. Songa, M. Y. and D. K. Kimb, S. M. Jo, D. Y. Kim, “Enhancement of the photocurrent generation in dye-sensitized solar cell based on electrospun TiO2 electrode by surface treatment”, Synthetic Metals , vol. 155, pp. 635–638, 2005

99. Jin, H. and Y. Hou, X. Meng, Y. Li, Q. Shi, F. Teng, “Enhanced photovoltaic properties of polymer–fullerene bulk heterojunction solar cells by thermal annealing”, Solid State Communications, vol. 142, pp. 181–184, 2007

100. Tang, W. L. and O. Park, “The effect of different heat treatments on the luminescence efficiency of polymer light-emitting diodes”, Adv. Mater., vol. 12, no. 11, pp. 801-804, 2000

101. “Flexographic ink containing a polymer or copolymer of a 3,4-dialkoxythiophene”, US Patènt 6890584, Agfa-Gevaert (Mortsel, BE), Appl. no. 175948, June 20, 2002

REFERENCES NOT CITED

Gutmann, F., Lyons, L.E., *Organic Semiconductors*, Berkeley, 1967.

Li, Z., Meng, H., *Organic Light-Emitting Materials and Devices*, CRC Press, 2007.

Bergh, A.A., Dean, P.J., *Light-emitting diodes*, Clarendon Press, Oxford, 1976.

Nilsson, D., *An Organic Electrochemical Transistor for Printed Sensors and Logic*, Norrköping, 2005.

Stark, P., Westling, D., *OLED-Evaluation and clarification of the new Organic Light Emitting Display technology*, Norrköping, 2002.

Roichmann, Y., *Charge Transport in Conjugated Polymers, Israel Institute of Technology*, Haifa, 2004.

Shinar, J., *Organic Light-Emitting Devices: A Survey*, Springer, AIP press, New York, 2004.

Tanase, C., *Unified charge transport in disordered organic field-effect transistors and light-emitting diodes*, University of Groningen, 2005.

APPENDIX

Machine code for the PIC16f877 microcontroller to drive passive matrix display.

```
0000: 2805 3FFF 3FFF 3FFF 3FFF 1683 0188 0187
0008: 1283 300A 00A8 300F 00A9 20B6 20F2 20D4
0010: 2110 212E 2020 203E 205C 2098 205C 207A
0018: 216A 214C 20B6 20F2 20D4 2110 212E 2809
0020: 0828 00A4 0828 00A3 3080 0087 307F 0088
0028: 2188 0C87 3049 0088 2188 0C87 3049 0088
0030: 2188 0C87 3049 0088 2188 0C87 3036 0088
0038: 2188 0BA3 2824 0BA4 2822 0008 0828 00A4
0040: 0828 00A3 3080 0087 307F 0088 2188 0C87
0048: 3040 0088 2188 0C87 3040 0088 2188 0C87
0050: 3040 0088 2188 0C87 303F 0088 2188 0BA3
0058: 2842 0BA4 2840 0008 0828 00A4 0828 00A3
0060: 3080 0087 307F 0088 2188 0C87 3002 0088
0068: 2188 0C87 3004 0088 2188 0C87 3002 0088
0070: 2188 0C87 307F 0088 2188 0BA3 2860 0BA4
0078: 285E 0008 0828 00A4 0828 00A3 3080 0087
0080: 3026 0088 2188 0C87 3049 0088 2188 0C87
0088: 3049 0088 2188 0C87 3049 0088 2188 0C87
0090: 3032 0088 2188 0BA3 287E 0BA4 287C 0008
0098: 0828 00A4 0828 00A3 3080 0087 307F 0088
00A0: 2188 0C87 3049 0088 2188 0C87 3049 0088
00A8: 2188 0C87 3041 0088 2188 0C87 3041 0088
00B0: 2188 0BA3 289C 0BA4 289A 0008 0828 00A4
00B8: 0828 00A3 3080 0087 300F 0088 2188 0C87
00C0: 3000 0088 2188 0C87 3000 0088 2188 0C87
00C8: 3000 0088 2188 0C87 3000 0088 2188 0BA3
00D0: 28BA 0BA4 28B8 0008 0828 00A4 0828 00A3
00D8: 3080 0087 3008 0088 2188 0C87 3008 0088
00E0: 2188 0C87 3008 0088 2188 0C87 3008 0088
00E8: 2188 0C87 3008 0088 2188 0BA3 28D8 0BA4
00F0: 28D6 0008 0828 00A4 0828 00A3 3080 0087
00F8: 3008 0088 2188 0C87 3004 0088 2188 0C87
0100: 3002 0088 2188 0C87 3001 0088 2188 0C87
0108: 3000 0088 2188 0BA3 28F6 0BA4 28F4 0008
0110: 0828 00A4 0828 00A3 3080 0087 3008 0088
0118: 2188 0C87 3010 0088 2188 0C87 3020 0088
0120: 2188 0C87 3040 0088 2188 0C87 3080 0088
0128: 2188 0BA3 2914 0BA4 2912 0008 0828 00A4
0130: 0828 00A3 3080 0087 30F8 0088 2188 0C87
0138: 3000 0088 2188 0C87 3000 0088 2188 0C87
0140: 3000 0088 2188 0C87 3000 0088 2188 0BA3
0148: 2932 0BA4 2930 0008 0828 00A4 0828 00A3
0150: 3080 0087 30AA 0088 2188 0C87 3055 0088
0158: 2188 0C87 302A 0088 2188 0C87 3055 0088
```

0160: 2188 0C87 302A 0088 2188 0BA3 2950 0BA4
0168: 294E 0008 0828 00A4 0828 00A3 3080 0087
0170: 3055 0088 2188 0C87 302A 0088 2188 0C87
0178: 3055 0088 2188 0C87 302A 0088 2188 0C87
0180: 3055 0088 2188 0BA3 296E 0BA4 296C 0008
0188: 3001 00A0 3014 00A1 3014 00A2 0BA2 298E
0190: 0BA1 298C 0BA0 298A 0008 0829 00A5 3032
0198: 00A6 30C8 00B7 0BB7 299B 0BA6 2999 0BA5
01A0: 2997 0008 3FFF 3FFF 3FFF 3FFF 3FFF 3FFF
01A8: 3FFF 3FFF 3FFF 3FFF 3FFF 3FFF 3FFF 3FFF